UCRL-16577

University of California

Ernest O. Lawrence Radiation Laboratory

TWO-WEEK LOAN COPY

This is a Library Circulating Copy
which may be borrowed for two weeks.
For a personal retention copy, call
Tech. Info. Division, Ext. 5545

ENERGY LEVELS OF ^{237}Np: II. HIGH RESOLUTION STUDY OF TRANSITIONS IN THE DECAY OF ^{237}U

Berkeley, California

DISCLAIMER

This document was prepared as an account of work sponsored by the United States Government. While this document is believed to contain correct information, neither the United States Government nor any agency thereof, nor the Regents of the University of California, nor any of their employees, makes any warranty, express or implied, or assumes any legal responsibility for the accuracy, completeness, or usefulness of any information, apparatus, product, or process disclosed, or represents that its use would not infringe privately owned rights. Reference herein to any specific commercial product, process, or service by its trade name, trademark, manufacturer, or otherwise, does not necessarily constitute or imply its endorsement, recommendation, or favoring by the United States Government or any agency thereof, or the Regents of the University of California. The views and opinions of authors expressed herein do not necessarily state or reflect those of the United States Government or any agency thereof or the Regents of the University of California.

UCRL-16577

UNIVERSITY OF CALIFORNIA

Lawrence Radiation Laboratory
Berkeley, California

AEC Contract No. W-7405-eng-48

ENERGY LEVELS OF ^{237}Np:
II. High Resolution Study of Transitions in the Decay of ^{237}U

T. Yamazaki and J. M. Hollander

January 1966

ENERGY LEVELS OF ^{237}Np:
II. High Resolution Study of Transitions in the Decay of ^{237}U

T. Yamazaki and J. M. Hollander

Lawrence Radiation Laboratory
University of California
Berkeley, California

RADIOACTIVITY ^{237}U; measured E_γ, I_γ, E_{ce}, I_{ce},; calc ICC; deduced ^{237}Np levels, J, π.

ENERGY LEVELS OF ^{237}Np:
II. High Resolution Study of Transitions in the Decay of ^{237}U

T. Yamazaki and J. M. Hollander

Lawrence Radiation Laboratory
University of California
Berkeley, California

January 1966

Abstract

The internal conversion electron and gamma-ray spectra from the decay of ^{237}U have been studied with use of a high-resolution $\pi\sqrt{2}$ iron-free spectrometer and solid-state gamma-ray spectrometers. In addition to the previously known transitions, several new lines were observed and fitted into the ^{237}Np level scheme. Absolute conversion coefficients for most of the transitions were determined. The presence of the previously undiscovered level at 281.35 keV, confirmed by the observation of a very strong 13.81 keV M1-E2 transition and a weak 221.8 keV crossover transition, establishes that the 267.54 keV 3/2- level is the lowest member of a K = 1/2- band.

1. Introduction

The continuing interest in the energy levels of $^{237}_{93}Np$ as an aid in the development of a nuclear model for the heavy elements has been pointed out in the introduction of the previous paper[1]), and in that paper a new analysis of the large body of data from $^{241}_{95}Am$ alpha decay is presented. Some of the many ^{237}Np levels seen in alpha decay are also populated by the beta decay of $^{237}_{92}U$, and these levels were the subject of an investigation in 1956 by Rasmussen, Canavan, and Hollander[2]). Although ^{237}U decay involves many gamma rays, most of which are too closely spaced to be resolved in scintillation spectra, the use of high-resolution permanent magnet spectrographs allowed RCH to make definite multipole assignments and to establish an unambiguous decay scheme.

Recently, two significant advances have made it worthwhile to re-study the decay of ^{237}U. One of these is the availability of lithium-drifted germanium and silicon detectors coupled to field-effect transistor preamplifiers ("FET"), with which gamma-ray line widths as small as 1 keV have been achieved. With these devices the photon spectra can be much better defined than was previously possible so that more accurate intensity measurements can be made and new, weak gamma rays can be identified. Also, in combination with high-resolution conversion electron spectroscopy, these detectors allow the determination of internal conversion coefficients for practically all transitions in the spectrum.

The other advance has been achieved in the new study of ^{241}Am by Lederer, Poggenburg, Rasmussen, Asaro, and Perlman[1]). Making use of the most recent advances in alpha decay theory[3]) together with new measurements of the gamma ray spectrum and alpha-gamma coincidences they proposed a level scheme

which involves a major reassignment of the ^{237}Np levels observed by Baranov, Kulakov, Zelenkov, and Shatinskii[4,5]) from their detailed ^{241}Am alpha spectrum data. Although the alpha decay of ^{241}Am involves many more levels than are seen from ^{237}U beta decay, the ^{237}U data are involved in an important way as a consequence of the fact that the 3/2- state at 267.5 keV, which receives most of the primary ^{237}U beta decay, has been assigned by LPARP as the I = 3/2 member of an inverted K = 1/2 band, with the I = 1/2 member assumed to have been unseen. From the known energies of the levels assigned by LPARP to the I = 5/2, 7/2, 9/2, and 11/2 members of this band, they predicted that the I = 1/2 level lies at ~280 keV. A consequence of this interpretation is the prediction that the I = 1/2 (280 keV) level is actually populated to a considerable extent from ^{237}U beta decay, but because it lies so close to the I = 3/2 level (267 keV) it has thus far escaped detection. A crucial test of this hypothesis is the search in ^{237}U decay for a strong low-energy intraband (1/2 → 3/2) transition (~13 keV) and also for the weak interband transition of ~221 keV proceeding to the 59.5 keV level. The experiment whose results are reported here was stimulated partly by this prediction, and partly by the desire to make accurate determinations of the internal conversion coefficients and multipole mixing ratios for ^{237}U decay. A preliminary report of the latter measurements had appeared[6]) prior to the work of LPARP and it is interesting that a weak 221 keV gamma ray had already been reported in that note.

In this paper we discuss our measurements of the transitions in ^{237}U, made with several solid-state gamma-ray spectrometers and the Berkeley 50-cm iron-free spectrometer. The predicted new level has been found, and its properties are in conformity with the level assignments of LPARP. Conversion

coefficients and multipole mixing ratios have been determined for most of the transitions, including the well-known 59.5 and 26.3 keV "anomalous" E1 transitions, and these are discussed in the following sections.

2. Source Preparation

The ^{237}U sources for gamma-ray and electron spectroscopy were produced by a high-flux ($\sim 5 \times 10^{15}$ n cm^{-2} sec^{-1}) irradiation of approximately 500 micrograms of ^{236}U at the Savannah River Plant, Savannah River, S. C. The integrated neutron flux (nvt) was approximately 6.3×10^{21} cm^{-2}. After dissolution of the target in a HCl-HNO_3 mixture and addition of Br_2 water to keep the uranium in the +6 oxidation state, the separation of uranium from neptunium and fission products was effected by a procedure using three progressively smaller Dowex-1 anion exchange columns. With uranium loaded on the column, washes were made with 6N HCl-HNO_3, 6N HCl-0.3N HF, and 4.3 N HCl. Removal of the uranium was done with 0.1 N HCl-0.06 N HF or with 0.1 N HCl.

Two sources were prepared for electron spectroscopy, by vacuum sublimation of the dried chloride solution from a shaped tungsten boat through a 1×10 mm^2 platinum collimator onto an aluminum foil backing of surface density ≈ 3.5 mg/cm^2. The first source deposit, practically invisible to the eye, was used for the scans of the low energy region of the internal conversion spectrum. The estimated disintegration rate of this source was $\approx 2 \times 10^8$ min^{-1}. The second source which had a visible deposit and a strength about ten times greater than the first, was used for the study of the high energy (>60 keV) conversion lines. Sources for gamma-ray spectroscopy were prepared in a variety of strengths, on non-metallic (Teflon) backings.

3. Gamma-Ray Spectroscopy

Gamma-ray measurements were carried out with three semiconductor spectrometers, described in table 1. With spectrometer A, the best detector available when the measurements began, the 332.4 keV-335.4 keV doublet was partially resolved. Subsequently, a new spectrometer (B), employing a field-effect transistor preamplifier[7]), was put into use, with sufficiently high resolution that the doublet could be resolved almost completely. Not only is the resolution of spectrometer B better but also it possesses higher efficiency than spectrometer A, since it can tolerate a much higher bias voltage on the crystal without increasing the noise level. Figure 1 shows a gamma-ray spectrum above 150 keV taken with spectrometer B. In order to reduce the total counting rate a lead absorber of 400 mg/cm^2 thickness was used. A number of repeated scans of the gamma spectrum showed no evidence of any gamma rays other than those indicated in the figure.

Spectrometer C, which consists of a 5 mmΦ × 3 mm thick Si(Li) crystal connected to an FET preamplifier, was successfully applied to the measurement of low-energy gamma rays and x rays. Figure 2 shows a gamma-ray spectrum in the low-energy region taken with this Si(Li) spectrometer. Also shown is a spectrum of ^{241}Am, by comparison with which the ^{237}U spectrum revealed the presence of a weak 51.0 keV gamma ray superimposed on the broad back-scattering peak associated with the strong 59.5-keV line. In addition to the three principal L x-ray groups the lowest member, L_ℓ, is seen at 11.9 keV.

The efficiency calibration curves for the three spectrometers were obtained by using the following sources with known absolute disintegration rates: ^{241}Am (59.5 keV), ^{57}Co (14.4 keV, 122.0 keV, 136.4 keV), ^{203}Hg (279.2 keV)

and ^{198}Au (411.8 keV), and by using radioisotopes with two or more radiations of known relative intensities, such as ^{241}Am, ^{203}Hg, ^{198}Au, ^{188}Re, ^{160}Tb, ^{109}Cd, and ^{57}Co. The relative intensity data used for the efficiency determinations are given in table 2. These efficiency calibrations demonstrated the superiority of the Si(Li) spectrometer over the Ge(Li) spectrometers for low-energy gamma-ray spectroscopy. As the gamma-ray energy decreases, the photopeak efficiency of the Ge(Li) spectrometers starts to drop rapidly at ~65 keV, while that of the Si(Li) spectrometer continues to increase, as illustrated in fig. 3.

The gamma-ray measurements from the three detectors are summarized in table 3, and averaged values of these gamma-ray intensities are subsequently used for the determination of internal conversion coefficients.

4. Conversion-Electron Spectroscopy

Portions of the internal conversion electron spectrum were studied with the Berkeley 50-cm $\pi\sqrt{2}$ iron-free spectrometer[10]). This instrument, utilizing a two-coil magnet system, is similar to the Uppsala instrument described by Siegbahn et al.[11]). Recently the focusing properties of the Berkeley spectrometer were substantially improved by the addition of a set of trim-coils[12]).

The automatically controlled cooling system, employing liquid Freon-11 as coolant, maintains temperature constancy within $\pm 0.5^{\circ}$C. The degaussing system consists of a four-coil Lee-Whiting array[13]) for the vertical component and pairs of Helmholz coils for the north-south and east-west components; with this system the vertical component of the residual field is $\leq 10^{-4}$ gauss along the electron optical path. (The iron-free building that houses the spectrometer

is located sufficiently far from the Bevatron that the residual pulsing field from this source is also $< 10^{-4}$ gauss.)

The spectrometer utilizes a transistor rectifier and regulator system that provides very good current stability, usually ~1:10^5. Scanning of the electron spectrum is done automatically from a preset starting current; both the current steps and the counting times can be varied over a wide range. The output data are recorded by an electric typewriter. Absolute values of the spectrometer magnet current are monitored manually by measuring the voltage drop across precision resistors with use of a Guildline type 9144 potentiometer.

The spectrometer is equipped with a set of interchangeable baffles to permit variations in the instrumental resolution. In scanning most of the ^{237}U electron lines the baffle permitting 0.06% momentum focusing aberration (aperture ≈ 0.25% of 4π) was used. Because of additional contributions to the line width from the finite source and counter dimensions, most lines had measured momentum widths of 0.07-0.08%. The low-energy lines were additionally broadened because of source-thickness up to 0.25% for the lowest energy line studied (8.1 keV).

For the study of low energy electrons, a pre-accelerator system was used in an attempt to avoid the uncertainties in intensity measurements caused by counter window absorption. This system was described by Cooper et al.[14]) and is shown schematically in fig. 4. The accelerating voltage, calibrated by direct measurements of the energy shifts of the 59.5 keV L_{II} line and the 33.2 keV L_I line, was 4.61±0.02 kV. Use of this system, however, was found also to introduce an uncertainty into the intensity measurements because of the focusing effect of the accelerating field, an effect that is evidently

quite energy dependent. Fortunately, just after the first scan of the low-energy ^{237}U lines, construction was finished on a "post-accelerator" G-M counter, which does not affect the spectrometer transmission, and with this detector it was possible to calibrate the intensity scale and make appropriate corrections to the intensity values measured with the preaccelerator device. These corrections amounted, at most, to 33% for the lowest electron energy studied (8.1 keV).

The detector used for these measurements was a side window G-M counter with a window aperture 1×38 mm^2, covered with a multi-layer formvar film of estimated surface density ≈ 60 μg/cm^2. The counter background was 15-20/min.

A continuous scan of the electron spectrum was not made because photographic recording spectrographs that covered the full energy range were utilized by RCH in their study of the ^{237}U electron spectrum, and it is unlikely that lines of appreciable intensity above ~15 keV would have been overlooked. Rather, an effort was made to measure with higher accuracy than had before been possible the energies and intensities of selected, important lines, especially in the energy region below 25 keV. As internal standards with which the momenta and intensities of other lines could be compared, the K- and L-lines of the 208.0 keV transition were measured several times during the course of the experiment. An absolute momentum scale was established with reference to the K and L_{III} lines of the 411.795±0.009 keV transition from ^{198}Au[15]). Calibration of the spectrometer is facilitated by use of a source holder that accommodates two sources so that the reference and "unknown" source can be moved alternately into the electron-optical source position without removing the source holder from the spectrometer.

For the measurement of internal conversion coefficients, the ^{198}Au sources also served as a calibration standard for the normalization of the electron intensities determined with the iron-free spectrometer and the photon intensities determined with the Ge(Li) spectrometers. This normalization is discussed further in Section 7.

The conversion electron intensity analysis was done by plotting the lines initially on a linear scale, subtracting an appropriate background function, then replotting the lines on semi-log paper. The line shapes on the semi-log plot are, over small energy regions, independent of line intensity, and thus the shapes of clearly resolved lines can be utilized to analyze unresolved groups. Integration of the line areas consisted in summing the counting rates down to 1% of the peak rate; assignment of errors in this procedure was done in the manner described by Novakov and Hollander[16].

Some examples of the measured conversion lines are shown in figs. 5 through 12.

5. Transition Energies and Electron Binding Energies

Many of the same low energy transitions from ^{237}U beta decay also occur in the alpha decay of ^{241}Am. A study of the internal conversion spectrum from the latter isotope has recently been reported by Wolfson and Park[17], and it is interesting to compare the results of the two investigations because iron-free spectrometers were used in both cases, with comparable instrumental resolutions and small limits of error. There are significant differences, too. For example, different methods of calibration were used; also, problems caused by alpha recoil effects of ^{241}Am are absent in the ^{237}U study.

In our study of the ^{237}U electron spectrum, two independent methods of spectrometer calibration were employed, each of which is capable of yielding high accuracy. In the first, the momentum ratios of the K and L_I lines of the 208 keV transition were carefully determined relative to the K and L_{III} lines of the 412-keV transition of ^{198}Au, and in the subsequent scans, which involved two different sources and several removals of the source holder, the K- and L_I-208 line were frequently remeasured as internal standards. With this mode of calibration, the energy of the L_I 59.5 line was found to be 37.112 ± 0.005 keV.

It is also possible, with a completely internal calibration, to determine the energy of the L_I 59.5 line, by utilizing the measured momentum ratio of two conversion lines of this transition (e.g., M_{II}/L_I current ratio) together with the knowledge of the energy difference between the lines. As discussed by Siegbahn[18]), this method is capable of yielding high accuracy with iron-free spectrometers provided that the atomic level separation is known with sufficient precision; the situation is favorable in this case, because the L_I-M_{II} level separation is given in the table of Bearden and Burr[19]) with a probable error of only 0.5 eV. With this calibration method, the energy of the L_I 59 line was found to be 37.114 keV. The agreement between the results of the two calibrations is very good (deviation ~5:10^5).

From our conversion line data and the known cascade-crossover relation involving the 59.5, 33.2, and 26.3 keV transitions, we can compute the absolute energy of the 59.5 keV transition from the following relationship:

$$E_{\gamma 59} = E_{\gamma 26} + E_{\gamma 33}$$

$$= (E_{L_I 59} - E_{L_I 33}) + (E_{M_I 59} - E_{M_I 26})$$

$$= 59.543 \pm 0.015 \text{ keV} \quad .$$

The transition energy so obtained agrees very closely with the value 59.545 ± 0.031 obtained by Wolfson and Park[17]) from a "Siegbahn-method" internal calibration in ^{241}Am decay. However Wolfson and Park chose not to use their own value for the final spectrometer calibration but rather to use the bent-crystal value of Day[20]), 59.568±0.017 keV. Although the three values agree within the combined errors, we believe that the probable error of Day's value has been underestimated.

A summary of our measured transition energy, intensity, and multipolarity data is presented in table 4. The intensity values have been normalized to an absolute percentage scale, as discussed in the following sections.

With use of the absolute transition energies and our measured electron line energies, we can compute the atomic binding energies of electrons in the K, L, M, and N shells of neptunium (Z=93). It is of interest to compare the values so calculated with the results of Wolfson and Park obtained in a similar manner from ^{241}Am, and with the values from x-ray spectroscopy given in the tables of Bearden and Burr[19]) and of Hagström et al.[21]). This comparison is given in table 5. It is seen that the agreement is generally quite good between our results and those of Wolfson and Park, obtained also from internal conversion spectroscopy, but that a comparison of the x-ray results with the internal conversion results shows only marginal agreement, the internal conversion results being systematically higher. This circumstance was also noted in the case of plutonium (Z=94), by Ewan, Geiger, Graham, and MacKenzie[22]).

6. Level Scheme

The levels of ^{237}Np that arise from ^{237}U beta decay have been discussed extensively by RCH, and we shall not repeat that discussion here except to the extent necessary to introduce new information obtained in this study. A level scheme incorporating all of our measured energy and intensity data on ^{237}U decay is shown in fig. 13. All observed transitions except that of 114.1 keV are placed in this scheme. In constructing the scheme, we noted that the balance of transition intensities is very good for each of the first five levels, consequently we have normalized all the photon and electron intensities absolutely to 100 ^{237}U beta disintegrations. The intensities of table 4 are so normalized, as are the photon abundances (given in parentheses) in the level scheme of fig. 13.

The major change in the ^{237}Np level scheme is the observation of the new level which was predicted by LPARP to lie at ≈280 keV. The level was readily established at 281.35±0.03 keV from the following sum and difference information:

$$(221.80\pm0.04) + (59.54\pm0.015) = 281.34\pm0.04$$

$$(208.00\pm0.023) + (59.54\pm0.015) + (13.81\pm0.03) = 281.35\pm0.04$$

$$(332.36\pm0.04) - (51.01\pm0.03) = 281.35\pm0.05$$

The knowledge of the multipolarities of the 13.81 (M1+E2), 221.80 (E2), and 51.01 (E1) keV transitions (see sections 8-10) confirms their placement in the scheme and also defines the spin and parity of the 281.35 keV level as 1/2-.

We note that the two E1 transitions (51.01 and 64.83) that depopulate the 332.36 keV (D 1/2+) level are the only E1 transitions observed from band D. Specifically, no E1 transitions are seen from levels D 5/2+ or D 3/2+. This fact can be understood from the competitive de-excitation modes available to these states. The higher levels, D 5/2+ and D 3/2+, can decay to band A via predominantly M1 transitions, while the lowest level, D 1/2+, can decay to band A only via an E2 transition, with which the E1 transitions can compete.

7. Determination of Absolute Conversion Coefficients

From the data on the relative intensities of gamma rays and conversion electrons one can derive the internal conversion coefficients (ICC) of all transitions provided that the ICC of at least one gamma ray is well known. In the ^{237}U study, the 208 keV transition makes an ideal conversion coefficient standard, because of its high intensity in both the electron and photon spectra. We have used two independent methods to determine the absolute conversion coefficients of the 208-keV transition. The first method is the comparison of the electron-to-gamma ratio of the 208-keV transition with that of the 412-keV transition of ^{198}Au. Using the accepted value

$$\alpha_K\,(412,\ ^{198}Au) = 0.0302 \pm 0.0005 \qquad \text{(Ref. 23)}$$

one can determine $\alpha_K\,(208,\ ^{237}U)$ with use of the relation

$$\alpha_K\,(208,\ ^{237}U) = \alpha_K\,(412,\ ^{198}Au)\ \frac{I_K\,(208,\ ^{237}U)}{I_K\,(412,\ ^{198}Au)}\ \frac{I_\gamma\,(412,\ ^{198}Au)}{I_\gamma\,(208,\ ^{237}U)}$$

The relative K line intensities were obtained with the iron-free spectrometer and the relative gamma-ray intensities were determined by using the two Ge(Li) spectrometers. Our result is: α_K (208, ^{237}U) = 2.30±0.12. The error in this value arises almost entirely from the uncertainty in the photoefficiency ratio $\epsilon(208)/\epsilon(412)$ for the Ge(Li) detectors.

The second method makes use of the relation

$$\frac{I(Kx)}{I_\gamma\ (208)} = \omega_K \cdot \alpha_K\ (208) \quad ,$$

where ω_K is the K fluorescence yield. The use of this relation implies the assumption that all the observed K x rays are associated with the conversion of the 208 keV transition, a good assumption in this case because of the predominance of the 208 keV transition (see table 4). The total K x-ray intensity is obtained by summing the intensities of the individual groups given in table 3. We obtain

$$\alpha_K\ (208) = 2.50 \pm 0.25$$

The two values for α_K (208) agree within experimental error. Because of its higher precision, we shall adopt the former value for the normalization of electron and gamma-ray intensity scales. With this normalization, the calculation of ICC for all the other ^{237}U transitions is straightforward, and the results are tabulated in column 7 of table 4. The quoted errors in the calculated ICC reflect principally the uncertainties of the gamma-ray intensities. Conversion coefficient ratios obtained from the conversion electron data are in general much more accurate, as can be seen from column 6 of the table.

8. Multipolarity Assignments of the High Energy Transitions

Figure 14 illustrates the comparison of the experimental K-conversion coefficients, α_K, with the theoretical values of Sliv and Band[24]). The α_K (208) agrees with the theoretical value for pure M1, with, of course, allowance for a small E2 admixture. To determine the E2 admixture precisely, the L subshell conversion coefficients are quite useful. Shown in fig. 15 are the theoretical conversion coefficients for K, L_I, L_{II}, and L_{III} shells versus percentage E2 photon admixture. The value (2.1±0.2)% E2 admixture is consistent with all the experimental data for the 208 keV transition.

The experimental α_K values for the 335.4-, 368.6-, and 370.9-keV transitions agree with the theoretical values for pure M1. The experimental errors are consistent with a maximum of 15% E2 admixture in each of these transitions.

The 332.4-keV transition is definitely assigned as pure E2. The 221.8-keV and 337.7-keV transitions are required from the decay scheme to be E2, and in fact, $\alpha_{L_{II}}$ (221.8) shows agreement with the theoretical E2 value. The α_K of the 164.6-keV transition, also required from the level scheme to be E2, is appreciably lower than theoretical, but on the other hand, all the L subshell conversion coefficients agree with theoretical for pure E2. The α_K (164.6) may be suspect because the "strong" ^{237}U source was used to record these lines, and at the energy of the K line considerably tailing due to source thickness was observed. Thus the line shape analysis is less certain than those of the higher energy K-lines.

The comparison between the experimental and theoretical conversion coefficients for the pure E2 transitions is given in table 6.

The K-conversion coefficient of the 234.4-keV transition agrees with the theoretical value for pure M2, which is consistent with the established decay scheme. The 267.5-keV transition shows a very high K-conversion coefficient compared to the theoretical value for pure E1. This high experimental K-conversion coefficient can be interpreted in terms of a 20±1% M2 photon admixture, if it is assumed that the conversion coefficients of the E1 and M2 components are normal (Sliv and Band theoretical values). Alternatively, an anomalously high conversion coefficient of the E1 component could be responsible for the experimental result. This point is discussed further in sect. 11.

9. Conversion Coefficients and Anomalies of E1 Transitions

The 26.35-keV and the 59.54-keV E1 transitions, which de-excite the 59.54-keV level (B 5/2-) to the 33.20-keV level (A 7/2+) and to the ground state (A 5/2+), respectively, are well known because of their anomalously high conversion coefficients, as discussed in detail by Asaro, Stephens, Hollander, and Perlman[25]). The absolute conversion coefficients and subshell conversion ratios obtained in the present work are compared with the theoretical values in table 7. The Sliv-Band L-subshell values are used except for L_{III}-26.35; for the L_{III} and M subshells of the 26.35-keV transition the quoted theoretical values were obtained from the table of Rose[26]) and from the threshold values around 30 keV, given by O'Connell and Carroll[27]). These values are for an unscreened, point nucleus. Roses's theoretical values are also used for the M subshells of the 59.54-keV transition. Our absolute values for the 59.54 L-subshell conversion coefficients agree with those obtained by Asaro et al.[25]), as shown in the

table, and the L-subshell conversion ratios are also in good agreement with the recent values of Wolfson and Park[17]). One can say that the anomalies in the 26.4- and 59.5-keV transitions are now quantitatively well established: (1) for the 59.5 keV transition $\alpha_{L_{III}}$ agrees with the theoretical value within the experimental error of 15%. $\alpha_{M_{III}}$ also agrees with theory for both 59.5 and 26.4-keV transitions, but there is an additional uncertainty in the theoretical M-shell values; (2) $\alpha_{L_{II}}$ (59.5) is higher than theoretical by the factor 3.8±0.6, and $\alpha_{M_{II}}$ (59.5) by about the same factor; (3) α_{L_I} (59.5) is higher than theoretical by the factor 1.8±0.3 and α_{M_I} (59.5) by about the same factor; (4) $\alpha_{M_{II}}$ (26.4) and α_{M_I} (26.4) are higher than theoretical by factors of about 2.2 and 1.6, respectively; (5) the N-subshell conversion shows anomalies similar to those in the M- and L-subshells.

The 51.01 and 64.83 keV transitions are unambiguously placed in the level scheme from the energy-sum relationships; they proceed from the 332.36-keV level (D 1/2+) to the 281.35 keV level (C 1/2-) and to the 267.54 keV level (C 3/2-), respectively. The experimental conversion coefficients demonstrate that these are E1 transitions, as expected from the level scheme. It was interesting to see if any anomalies would be found in their conversion coefficients; the data as summarized in table 8 show no significant deviations from the theoretical values, although the experimental errors are large in these cases.

10. E2 Admixture in the 13.81 keV Transition

It is of interest to derive the M1/E2 mixing ratio of the 13.81 keV intraband transition, but there are no readily applicable theoretical M-subshell conversion coefficients with which to do this. The theoretical M-subshell coefficients of Rose[26]), calculated for an unscreened point nucleus, extend only down to 25.6 keV. Recently, O'Connell and Carroll[27]) calculated conversion coefficients near threshold (around 15 keV in Np) for an unscreened point nucleus. With the aid of these we estimated the theoretical M-subshell coefficients, which are given in columns 3 and 4 of table 9. From the experimental M_I, M_{II}, and M_{III} subshell ratios we obtain a fairly consistent value of the mixing ratio, ~0.15% E2. With the assumption of Q_0 = 12 barns for this band, we calculate from this mixing ratio $|g_\Omega - g_R| \times (1 + b_0) \approx 2.2$, where b_0 is the decoupling parameter for the M1 transition[28]). This value is similar to those from the other rotational bands[29]).

The E2 admixtures of other intraband transitions are given in table 4.

11. Interband Transitions and Band Mixing

In the work of RCH, the bands A, B, and D were given Nilsson assignments of 5/2+[642], 5/2-[523], and 1/2+[400], respectively. As discussed earlier, band C, thought to be K = 3/2 by RCH, has been reassigned by LPARP as the Nilsson state 1/2-[530], and this work has confirmed that assignment.

The de-excitation spectrum of the 267.54 keV level (C 3/2-) is interesting because the four multipoles E1, M1, E2, and M2 are all observed. Some further comments should be made about their transition rates because of the level reassignments. Table 10 presents a summary of our data on the absolute

rates of these transitions, calculated from our intensities and mixing ratios, with use of the measured half-life of this state, 5.4 ns[30]). Hindrance factors are given for all six multipole components, and in the last column the squares of appropriate Clebsch-Gordan coefficients are listed; the ratios of the hindrance factors are expected to be proportional to the Clebsch-Gordan ratios if the bands are pure in the K quantum number.

The large retardation of the E1 and M1 transitions is now readily understood in terms of the K-forbiddenness of these transitions.

In the case of the E2 and M2 transitions, large discrepancies are found between the experimental hindrance factor ratios and the theoretical ratios for pure K. From our data we find

$$[F_{208}(E2)/F_{165}(E2)]_{exp} = 0.08 \quad ,$$

whereas the theoretical ratio for $K_i = 1/2$ and $K_f = 5/2$ is

$$[F_{208}(E2)/F_{165}(E2)]_{theor} = 1.33 \quad .$$

E2 single proton transitions between the C and B bands violate the asymptotic selection rule $\Delta\Lambda = \pm 1$, thus we may consider the possibility of contributions to the E2 transition rates from $K = 3/2$ admixtures, such as are necessary to explain the K-forbidden M1 and E1 transitions. If the E2 transitions were to take place entirely via a Coriolis admixed $K = 3/2$ component, the transition amplitudes would be proportional to the Clebsch-Gordan coefficients multiplied by the Coriolis admixing amplitude $\sqrt{(I-K)(I+K+1)}$. Then the theoretical ratio would be

$$K_i = 1/2,\ K_f = 3/2:\quad [F_{208}(E2)/F_{165}(E2)]_{theor} = 0.021 \quad \text{or}$$

$$K_i = 3/2,\ K_f = 5/2:\quad [F_{208}(E2)/F_{165}(E2)]_{theor} = 0.75 \quad .$$

depending on whether the admixture is in the final or initial state. The first alternative provides better agreement with the experimental value. Possible K = 3/2 Nilsson orbitals that have Coriolis matrix elements with the 5/2-[523] orbit are 3/2-[532] and 3/2-[521]. Unhindered E2 transitions can take place from the 1/2-[530] state to either of these states.

The situation with the M2 transitions is not as readily explained. Our data indicate

$$[F_{267}(M2)/F_{234}(M2)] = 3.7$$

whereas the theoretical ratio is 1.33. This discrepancy is only made larger by the admixture of K_i or $K_f = 3/2$. As pointed out by RCH, a possible explanation for the high experimental value might be the existence of anomalously high K conversion coefficient of the E1 component of γ_{267}. An anomaly factor of 13 would be required to bring the M2 branching ratio into agreement with theory. It is interesting to note that the most anomalous E1 transition presently known, the 84 keV transition in $^{231}_{91}Pa$[25,31]), takes place between two bands that have been given the same Nilsson assignments as bands C and A. In the case of ^{231}Pa, however, the 5/2+[642] band is considered to be very highly admixed.

Table 11 summarizes the experimental relative photon hindrance factors for the interband transitions from band D (K = 1/2+). Since dipole radiation from band D to band A (K = 5/2) is forbidden by the K-selection rule, interpretations of the data must be sought in terms of state admixtures. The M1

transitions from the 3/2+ member are comparable in strength to the 38.54 keV intraband transition, and should therefore have lifetimes of the order of 10^{-10} s, or about 10^{-2} single particle units. This is surprisingly fast, considering that these transitions are K-forbidden, and implies a rather large K = 3/2 admixture in band D or band A. The Nilsson band 3/2+[651] has large Coriolis matrix elements with the 5/2+[642] ground state band (A), and is therefore likely to be responsible for the strength of the M1 transitions. This band has not yet been observed in ^{237}Np.

The M1 branching ratios from the D 5/2+ level do not themselves determine whether mixing into band A or band D is responsible for the M1 transitions. If we multiply the Clebsch-Gordan coefficients by the spin-dependent part of the Coriolis admixing amplitude $\sqrt{(I-K)(I+K+1)}$ to obtain the transition amplitudes, then

$$[F_{369}(M1)/F_{335}(M1)]_{theor} = 0.40$$

for both of $K_i = 3/2$, $K_f = 5/2$, and $K_i = 1/2$, $K_f = 3/2$ cases, which agrees with the experimental value

$$[F_{369}(M1)/F_{335}(M1)]_{exp} = 0.37 \quad .$$

We note that the hindrance factors of the (D → A) E2 radiations are of the same order of magnitude as those of the M1 radiations, thus the E2 transitions must also be retarded. This is consistent with the fact that E2 transitions between these two bands violate the asymptotic selection rule $\Delta n_z = 0,1$. Although our experimental relative E2 transition probabilities are only approximate for the (D → A) radiations, they appear to agree with the theoretical values for $K_i = 1/2$ and $K_f = 5/2$.

12. ^{237}U Beta Decay and Spin-Parity Assignment

On the basis of beta decay branching and log ft information, RCH assigned spin 1/2 to the ground state of ^{237}U. A definitive parity assignment was not made, and it was noted that the properties of both the 1/2-[501] and 1/2+[631] Nilsson orbitals were probably consistent with the experimental beta decay data.

Recently four members of the ground state rotational band of ^{237}U have been observed in the alpha spectrum of ^{241}Pu by Baranov, Gadzhiev, Kulakov, and Shatinskii[32]). The ^{237}U spin of 1/2 was confirmed, and the experimental values of the rotational parameters were found to be $\hbar^2/2\mathfrak{J}$ = 6.4 keV and $\underline{a}$ = -0.44. Assignment of the band was made to the 1/2+[631] Nilsson orbital, which is also found as the ground state of ^{239}Pu and ^{241}Cm. In the case of ^{239}Pu, the rotational parameters are $\hbar^2/2\mathfrak{J}$ = 6.25 and $\underline{a}$ = -0.58 [22]). Evidence against the 1/2-[501] assignment, considered as an alternative for ^{237}U by RCH, is provided by the observed value of the decoupling parameter, -0.44, which is considerably closer to the theoretical value for state 1/2+[631], ~ -1, than to the value for state 1/2-[501], ~ +1 (see, for example, the systematic calculations of decoupling parameters of K = 1/2 bands presented by Valentin[33])).

Further evidence favoring the 1/2+[631] assignment is provided by the alpha-particle intensities found by Baranov et al.[32]) from ^{241}Pu decay. A strong alternation is found in the intensities of alpha groups populating the various members of the rotational band, which, according to the theoretical calculations of Poggenburg[3]) for states in ^{239}Pu, is a characteristic to be expected to be much more pronounced in the [631] band than in the [501] band.

It is interesting to consider our ^{237}U beta decay data with respect to the ^{237}U ground state assignment 1/2+[631]. The experimental log ft values

for beta decay to the 1/2 and 3/2 members of band C (1/2-[530]) are essentially equal (~6.5) and can be interpreted as first forbidden, unhindered, in accordance with the asymptotic selection rules of Alaga[34]). An important new piece of information, from the work of LPARP, is the knowledge of the energy of the 5/2- member of band C (357 keV). Beta decay population of this state would be detected by the observation of the intraband transition (5/2 → 3/2) at about 90 keV. RCH did not detect this transition, in their photographically recorded conversion electron spectrum, but it is difficult to set a meaningful lower limit to the log ft value of the corresponding beta transition from their data. It would be of interest to search for this state in a future study of ^{237}U, as its observation would be an important piece of corroborative evidence for the even parity assignment to ^{237}U.

Beta decays to the 1/2+ and 3/2+ members of band D (1/2+[400]) proceed via allowed transitions, but these would be expected according to the asymptotic selection rules to be highly hindered because of the change in oscillator quantum number $\Delta N = 2$. The observed log ft values (7.3 and 7.8 respectively) indicate retardations of about a factor of 100 from the "normal" rates for allowed transitions, which is consistent with the interpretation given.

In the de-excitation spectrum of ^{237}U, the 5/2+ member of band D (368.6 keV) is observed to be populated in about 0.25% of the ^{237}U beta decays. The direct beta decay from ^{237}U would be second-forbidden and unobservable, thus we must assume that the 368.6 keV state arises entirely via an unobserved 2.3 keV intraband transition (D 3/2+ → D 5/2+).

13. Acknowledgments

We wish to acknowledge with thanks the stimulating interest of Dr. C. M. Lederer in this experiment. The comments of Prof. J. O. Rasmussen are deeply appreciated. We wish also to thank J. A. Harris for his help in preparing the samples, and C. A. Butler for his assistance with the iron-free spectrometer. One of us (T.Y.) is deeply grateful to Professors I. Perlman and J. O. Rasmussen for their kind hospitality during his stay with the Nuclear Chemistry Division, and to the Miller Institute for Basic Research in Science of the University of California for the receipt of a Miller Research Fellowship.

References

1) C. M. Lederer, J. K. Poggenburg, F. Asaro, J. O. Rasmussen, and I. Perlman, preceding paper; referred to hereafter as LPARP.

2) J. O. Rasmussen, F. L. Canavan, and J. M. Hollander, Phys. Rev. 107 (1957) 141; this paper is referred to hereafter as RCH.

3) J. K. Poggenburg, Jr., Ph.D. Thesis, Lawrence Radiation Laboratory Report UCRL-16187, (August 1965)

4) S. A. Baranov, V. M. Kulakov, A. G. Zelenkov, and V. M. Shatinsky, Nucl. Phys. 43 (1963) 547

5) S. A. Baranov, V. M. Kulakov, and V. M. Shatinsky, Nucl. Phys. 56 (1964) 252

6) T. Yamazaki and J. M. Hollander, 1964 Nuclear Chemistry Division Annual Report, Lawrence Radiation Laboratory Report UCRL-11828, p. 31

7) E. Elad, Lawrence Radiation Laboratory Report UCRL-16390, (September 1965); Nucl. Instr. Methods, 37, 327 (1965)

8) L. B. Magnusson, Phys. Rev. 107 (1957) 161

9) Nuclear Data Sheets, Nuclear Data Group, Oak Ridge National Laboratory

10) K. Siegbahn, C. L. Nordling, and J. M. Hollander, 1961 Nuclear Chemistry Division Annual Report, Lawrence Radiation Laboratory Report UCRL-10023, p. 232

11) K. Siegbahn, C. Nordling, S.-E. Karlsson, S. Hagström, A. Fahlman, and I. Andersson, Nucl. Instr. Methods 27 (1964) 173

12) K.-E. Bergkvist and J. M. Hollander, Nucl. Instr. Methods (to be published)

13) G. E. Lee-Whiting, "Uniform Magnetic Fields", Chalk River Laboratory Report CRT-673 (February 1957)

14) J. A. Cooper, J. M. Hollander, M. I. Kalkstein, and J. O. Rasmussen, Nucl. Phys. 72 (1965) 113

15) G. Murray, R. L. Graham, and J. S. Geiger, Nucl. Phys. 63 (1965) 353

16) T. Novakov and J. M. Hollander, Nucl. Phys. 60 (1964) 593

17) J. L. Wolfson and J. J. H. Park, Can. J. Phys. 42 (1964) 1387

18) K. Siegbahn, in "Alpha-, Beta-, and Gamma-Ray Spectroscopy", North-Holland Publishing Co., Amsterdam, 1965, p. 193

19) J. A. Bearden and A. F. Burr, "Atomic Energy Levels", AEC Report NYO-2543-1 (1965)

20) P. P. Day, Phys. Rev. 97 (1955) 689

21) S. Hagström, C. Nordling, and K. Siegbahn, in "Alpha-, Beta-, and Gamma-Ray Spectroscopy", North-Holland Publishing Co., Amsterdam, 1965, Appendix 2, p. 845

22) G. T. Ewan, J. S. Geiger, R. L. Graham, and D. R. MacKenzie, Phys. Rev. 116 (1959) 950

23) S. Hultberg, et al., quoted in "Internal Conversion Processes", ed. by J. H. Hamilton, Academic Press, 1966

24) L. A. Sliv and I. M. Band, Coefficients of Internal Conversion of Gamma-Radiation (USSR Academy of Sciences, Moscow-Leningrad, 1956) Part I: K Shell, Part II: L-Shell; Gamma Rays, ed. by L. A. Sliv (USSR Academy of Sciences, Moscow-Leningrad, 1961)

25) F. Asaro, F. S. Stephens, J. M. Hollander, and I. Perlman, Phys. Rev. 117 (1960) 492

26) M. E. Rose, "Internal Conversion Coefficients", North-Holland Publishing Co., Amsterdam, 1959

27) R. F. O'Connell and C. O. Carroll, Phys. Rev. 138 (1965) B1042; "Internal Conversion Processes", ed. by J. H. Hamilton, Academic Press, 1966

28) G. Alaga, K. Alder, A. Bohr, and B. R. Mottelson, Kgl. Danske Videnskab. Selskab, Mat.-Fys. Medd. 29 (1955) No. 9

29) J. M. Hollander, W. G. Smith, and J. O. Rasmussen, Phys. Rev. 102 (1956) 1372

30) M. E. Bunker, J. P. Mize, and J. W. Starner, Bull. Am. Phys. Soc. 2 (1957) 104

31) J. M. Hollander, F. S. Stephens, F. Asaro, and I. Perlman, unpublished results quoted by E. K. Hyde, I. Perlman, and G. T. Seaborg, "The Nuclear Properties of the Heavy Elements", Vol. II, Prentice-Hall, Inc., Englewood Cliffs, New Jersey, 1964, p. 648

32) S. A. Baranov, M. K. Gadzhiev, V. M. Kulakov, and V. M. Shatinskii, Soviet Journal of Nuclear Physics 1 (1965) 557

33) J. Valentin, Nucl. Phys. 36 (1962) 549

34) G. Alaga, Nucl. Phys. 4 (1957) 625

Table 1
Gamma-ray spectrometers used in the ^{237}U measurements

		A	B	C
Crystal		Ge(Li)	Ge(Li)	Si(Li)
Size		1 cm × 2 cm × 5 mm thick	1 cm × 1 cm × 5 mm thick	5 mmϕ × 3 mm thick
Bias (volt)		240	900	390
Preamplifier		EC 1000	FET	FET
Resolution at (FWHM)	14 keV			0.97
	59 keV	2.4	1.5	1.17
	122 keV	2.4	1.6	1.27
	267 keV	2.5	1.7	

Table 2
Relative-intensity standards used to calibrate the gamma-ray spectrometers

Isotope	Photon energy[d] (keV)	Relative intensity	Method[a]
^{241}Am	11.9 Np L_{ℓ}	2.2	PROP[b]
	14.0 Np L_{α}	37.5	
	17.8 Np L_{β}	51.2	
	20.8 Np L_{γ}	13.8	
	26.35	7.0	
	59.54	100	
^{109}Cd	22.2 Ag K_{α}	25.5	SSD
	24.9 Ag K_{β}	5.5	
	87.7	1.00	
^{57}Co	14.4	11	SSD
	122.1	100	
	136.4	13	
^{188}Re	63.0 Os K_{α}	24.2	ICC
	71.4 Os K_{β}	6.6	
	155.0	100	
^{203}Hg	72.9 Tl K_{α}	11.9	ICC
	82.6 Tl K_{β}	3.44	
	279.2	100	
^{198}Au	70.8 Hg K_{α}	2.24	ICC
	80.3 Hg K_{β}	0.643	
	411.8	100	
^{137}Cs	32.2 Ba K_{α}	6.85	ICC
	36.4 Ba K_{β}	1.54	
	661.6	100	

Table 2. Continued

Isotope	Photon energy[d] (keV)	Relative intensity	Method[a]
^{180m}Hf	55.8 Hf K_α	25.2	ICC and DS
	63.2 Hf K_β	7.4	
	93.3	16.8	
	215.3	80.6	
	332.5	94.8	
	443.6	83.0	
	501.2	14.2	
^{160}Tb	46.0 Dy K_α	116	ICC
	52.1 Dy K_β	28.8	
	86.8	100	
^{22}Na	511.0	180	DS[c]
	1274.6	100	
^{60}Co	1173.2	100	DS[c]
	1332.5	100	
^{88}Y	898.2	93	DS[c]
	1836.2	99	
^{24}Na	1368.5	100	DS[c]
	2753.9	100	

[a]Abbreviated as follows: PROP—Proportional counter spectrometry; SSD—Solid-state detector spectrometry; ICC—Assuming K internal conversion coefficient of a pure E2 transition from negatron emitter, and use of K-fluorescence yield; DS—Well established from decay scheme.

[b]Reference 8

[c]Reference 9

[d]The quoted x-ray energies are $K\alpha_1$ and $K\beta_1$

Table 3
Summary of ^{237}U gamma-ray measurements

E_γ (keV)	Relative intensities			
	A Ge(Li)	B Ge(Li)	C Si(Li)	Adopted value
11.9 Np L_ℓ			6.5±0.7	6.5±0.7
14.0 Np L_α			115±12	115±12
17.8 Np L_β			122±12	122±12
20.8 Np L_γ			33±3	33±3
26.4			10.5±1.1	10.5±1.1
33.2			0.5±0.2	0.5±0.2
38.5, 43.4			<0.1	<0.1
51.0			0.98±0.44	0.98±0.44
59.5	155±16	158±16	155	155±16
64.9	5.0±0.4	5.4±0.5	5.9±0.6	5.4±0.6
97.0 Np K_{α_2}	77±8	76±8	76±8	76±8
101.0 Np K_{α_1}	99±10	112±11	106±11	106±11
113.5 Np K_{β_1}	48±4.8	44±4.4		46±4.6
117.5 Np K_{β_2}	15.4±1.5	14.0±1.4		14.6±1.5
164.5	8.26±0.40	8.67±0.40		8.46±0.25
208.0	100	100	100	100
221.8	0.087±0.005	0.101±0.006		0.094±0.006
234.5	0.092±0.005	0.088±0.006		0.090±0.006
267.5	3.36±0.010	3.27±0.06		3.29±0.06
292.7	0.010±0.002	0.014±0.003		0.012±0.003
332.4	5.80±0.30	5.48±0.22		5.55±0.22
335.4	0.45±0.02	0.44±0.03		0.44±0.03
337.8	0.032±0.010	0.038±0.005		0.035±0.005
368.6	0.241±0.020	0.197±0.012		0.215±0.015
370.9	0.508±0.030	0.516±0.031		0.512±0.031

Table 4
Summary of ^{237}U transition energies, intensities, and conversion coefficients

Transition	Transition energy (keV)	Photon[a] intensity (percent)	Shell	Electron[b] energy (keV)	Electron[a] intensity (percent)	Internal conversion coefficient	Multipolarity	Remarks
C 1/2- → C 3/2-	13.81±0.02		M_I	8.051±0.03	32.9±0.3		M1 + 0.15% E2	c
			M_{II}	8.431±0.03	5.14±0.11			c
			M_{III}	9.370±0.03	2.78±0.11			c
			M_{IV}	9.95	≤2.30			c
			M_V	10.14	≤1.44			c
			N_I	12.318±0.03	9.25±0.11			c
			N_{II}	12.479±0.03	1.87±0.11			c
B 5/2- → A 7/2+	26.348±0.010	2.41±0.24	L_{III}	8.75±0.03	3.64±0.11	1.48±0.19	E1	c
			M_I	20.601±0.012	0.952±0.070	0.387±0.065		
			M_{II}	20.974±0.012	1.58±0.12	0.65±0.10		f
			M_{III}	21.904±0.012	0.82±0.04	0.335±0.050		
			M_{IV}	22.49	0.18±0.02	0.074±0.014		
			M_V	22.67	0.34±0.02	0.137±0.022		
			N_I	24.839±0.013	0.29±0.02	0.118±0.020		
			N_{II}	25.017±0.013	0.57±0.02	0.231±0.030		
			N_{III}	25.254±0.013	0.22±0.02	0.089±0.018		
A 7/2+ → A 5/2+	33.195±0.011		L_I	10.764±0.005	11±1.1		M1 + 1.4% E2	c
			L_{II}	11.59±0.03	3.1±0.1			c
			L_{III}	15.59±0.03	2.1±0.1			c
			M_{III}	28.75±0.015	0.65±0.02			
D 3/2+ → D 1/2+	38.54±0.03		L_I	10.76	<0.04		E2/M1 >0.3	
			L_{II}	16.93±0.015	0.31±0.10			d
			L_{III}, M_{II}					e
			M_{III}	34.10±0.025	0.03±0.01			

Table 4. Continued

Transition	Transition energy (keV)	Photon[a] intensity (percent)	Shell	Electron[b] energy (keV)	Electron[a] intensity (percent)	Internal conversion coefficient	Multipolarity	Remarks
B 7/2- → B 5/2-	43.423±0.020		L_I	20.99	1.25±0.13		M1 + 14% E2	f
			L_{II}	21.811±0.012	1.66±0.03			
			M_I	37.67	0.53±0.03			
			M_{II}	38.05	0.67±0.03			
D 1/2+ → C 1/2-	51.01±0.03	0.22±0.10	L_I	28.59	0.059±0.016	0.26±0.20	E1	
			L_{II}	29.41	0.075±0.016	0.33±0.23		
			L_{III}	33.40±0.02	0.080±0.011	0.35±0.18		
B 5/2- → A 5/2+	59.543±0.015	36.0±3.6	L_I	37.112±0.005	8.67±0.16	0.240±0.029	E1	
			L_{II}	37.931±0.006	16.96±0.17	0.468±0.047		
			L_{III}	41.926±0.008	4.71±0.16	0.131±0.013		
			M_I	53.795±0.010	2.21±0.16	0.061±0.010		
			M_{II}	54.173±0.010	4.36±0.16	0.121±0.016		
			M_{III}	55.099±0.010	1.13±0.11	0.032±0.006		
			M_{IV}	55.68	0.19±0.05	0.0053±0.0020		
			M_V	55.869±0.020	0.24±0.05	0.0065±0.0020		
D 1/2+ → C 3/2-	64.83±0.02	1.25±0.13	L_I	42.39±0.015	0.123±0.016	0.098±0.023	E1	
			L_{II}	43.22±0.015	0.160±0.016	0.125±0.025		
			L_{III}	47.21±0.015	0.134±0.016	0.105±0.021		
not placed in the decay scheme	114.09±0.05		L_I	91.67±0.05	0.021±0.004			g
			L_{II}	92.47±0.05	0.021±0.004			g
			L_{III}	96.46±0.05	0.023±0.004			g
C 3/2- → B 7/2-	164.61±0.02	1.97±0.06	K	45.91±0.015	0.285±0.010	0.145±0.015	E2	
			L_I	142.17±0.026	0.127±0.006	0.065±0.010		
			L_{II}	143.01±0.026	1.34±0.02	0.680±0.060		
			L_{III}	146.99±0.026	0.68±0.01	0.348±0.030		

Table 4. Continued

Transition	Transition energy (keV)	Photon[a] intensity (percent)	Shell	Electron[b] energy (keV)	Electron[a] intensity (percent)	Internal conversion coefficient	Multipolarity	Remarks
C 3/2- → B 5/2-	208.005±0.023	23.3	K	89.337±0.013	53.5	2.30±0.12	M1 + 2.1% E2	
			L_I	185.569±0.025	9.82±0.10	0.42±0.02		
			L_{II}	186.398±0.025	1.39±0.01	0.060±0.03		
			L_{III}	190.383±0.025	0.108±0.003	0.0047±0.0002		
C 1/2- → B 5/2-	221.80±0.04	0.0219±0.0014	K	103.13	<0.01	<0.49	E2	
			L_I	199.36	<0.0007	<0.04		
			L_{II}	200.18±0.04	0.0044±0.0006	0.200±0.020		
			L_{III}	204.16±0.04	<0.004	<0.09		
C 3/2- → A 7/2+	234.40±0.04	0.0209±0.0014	K	115.74±0.04	0.140±0.006	6.73±0.40	M2	
C 3/2- → A 5/2+	267.54±0.04	0.765±0.014	K	148.88±0.04	0.596±0.004	0.776±0.038	E1 + 20% M2[i]	
D 5/2+ → A 9/2+	292.7 ±0.1[h]	0.0028±0.0007					[E2][j]	
D 1/2+ → A 5/2+	332.36±0.04	1.29±0.05	K	213.70±0.04	0.82±0.02	0.0635±0.0060	E2	
D 5/2+ → A 7/2+	335.38±0.04	0.102±0.007	K	216.72±0.04	0.059±0.002	0.575±0.060	M1 + <15% E2	
D 3/2+ → A 7/2+	337.7 ± 0.5[h]	0.0081±0.0012	K	219.0	<0.003	<0.37	E2[j]	
D 5/2+ → A 5/2+	368.59±0.04	0.050±0.003	K	249.93±0.04	0.027±0.001	0.545±0.060	M1 + <15% E2	
D 3/2+ → A 5/2+	370.94±0.04	0.119±0.007	K	252.28±0.04	0.053±0.002	0.446±0.050	M1 + <15% E2	

Table 4. Footnotes

[a]The quoted intensities are absolute values in percent of total ^{237}U beta decays, normalized according to the procedure described in section 6.

[b]The electron energy values quoted with errors are measured values, which were used for the determination of binding energies and transition energies. The values given without errors are from calculated line positions, which were used as an aid for the intensity determinations of weak lines.

[c]Measured with use of a preaccelerator. The quoted error in intensity does not include a possible systematic error of 10%.

[d]This line is part of an unresolved Auger group, and the quoted intensity may be too high.

[e]These lines are completely masked.

[f]$L_I 43.4$ and $M_{II} 26.3$ are unresolved; the intensity of each was evaluated with use of L_I/L_{II} 43.4 from Wolfson and Park.

[g]Photon masked by K_β x ray group.

[h]The energy was determined from the gamma-ray spectrum.

[i]The quoted mixing ratio is based on the measured K-conversion coefficient with the assumption of theoretical values for the E1 and M2 components. If, however, the E1 component is anomalously converted, the M2 component may be lower; see discussion (sec. 11).

[j]Required by the decay scheme.

Table 5
Atomic electron binding energies in neptunium (Z = 93)
(binding energies in keV, errors in eV)

	x-ray spectroscopy		Cascade-crossover relations (iron-free spectrometer)	
	Bearden and Burr[19])	Hagström et al.[21])	Wolfson and Park[17])	This work
K	118.674±33	118.660	---	118.663±31[a]
L_I	22.418±2	22.414	22.445±14	22.431±13
L_{II}	21.596±0.9	21.596	21.618±14	21.612±14
L_{III}	17.606±0.9	17.606	17.627±14	17.617±15
M_I	5.719±3.6	5.724	5.750±15	5.748±15
M_{II}	5.357±2.1	5.354	5.377±19	5.370±16
M_{III}	4.429±3.1	4.422	4.446±19	4.444±15
M_{IV}	3.847±0.9	3.847	3.858±19	---
M_V	3.662±0.9	3.666	3.670±19	3.674±24
N_I	1.476±18	1.490	1.506±23	1.509±16
N_{II}	1.308±18	1.318	1.334±23	1.331±16
N_{III}	1.079±18	1.076	1.093±25	1.094±16
N_{IV}	0.812±0.9	0.812	0.831±30	---
N_V	0.766±0.9	0.768	0.786±30	---
O	---	0.340	0.290±30	---
P	---	---	0.050±30	---

[a]Obtained from the K-L_I energy difference of the 208 keV transition and the L_I binding energy.

Table 6
Conversion coefficients of the pure E2 transitions

Transition energy (keV)	Shell	Conversion coefficients		
		Exp	Theor (Sliv-Band)	Exp/theor
164.61	K	0.145±0.015	0.188	0.77±0.08
	L_I	0.065±0.010	0.070	0.93±0.14
	L_{II}	0.680±0.060	0.72	0.95±0.08
	L_{III}	0.348±0.030	0.38	0.91±0.08
221.80	L_{II}	0.200±0.020	0.19	1.07±0.11
	L_{III}	<0.09	0.087	<1.1
332.36	K	0.0635±0.0060	0.063	1.00±0.10

Table 7
Conversion coefficients of the E1 transitions from band B to band A

Transition energy (keV)	Shell	Experimental		Theoretical		Exp/theor
		This work	Others	Sliv-Band	Rose[c]	
26.35	L_{III}	1.48±0.19	1.2[b]		1.75	0.82±0.10
(B 5/2- → A 7/2+)	M_I	0.387±0.065			0.250	1.55±0.26
	M_{II}	0.65±0.10			0.300	2.15±0.32
	M_{III}	0.335±0.050			0.400	0.84±0.12
	M_{IV}	0.074±0.014			0.168	0.44±0.09
	M_V	0.137±0.022			0.200	0.69±0.11
	M_I/M_{III}	1.16±0.12	1.2±0.2[a]		0.63	1.84±0.18
	M_{II}/M_{III}	1.93±0.19			0.75	2.60±0.26
	M_{IV}/M_{III}	0.22±0.03	0.44±0.13[a]		0.42	0.52±0.07
	M_V/M_{III}	0.41±0.04	0.37±0.11[a]		0.50	0.82±0.08
	N_I	0.118±0.020				
	N_{II}	0.231±0.030				
	N_{III}	0.089±0.018				
	N_I/N_{III}	1.32±0.28	1.0±0.35[a]			
	N_{II}/N_{III}	2.60±0.50	2.4±0.8[a]			
59.54	L_I	0.240±0.029	0.22±0.02[b]	0.134		1.79±0.21
	L_{II}	0.468±0.047	0.46±0.05[b]	0.124		3.80±0.38
	L_{III}	0.131±0.013	0.12±0.03[b]	0.126		1.04±0.11
	L_I/L_{III}	1.84±0.07	1.76±0.13[a]	1.06		1.74±0.07
	L_{II}/L_{III}	3.60±0.14	3.35±0.24[a]	0.98		3.67±0.14

Table 7. Continued

Transition energy (keV)	Shell	Experimental		Theoretical		Exp/theor
		This work	Others	Sliv-Band	Rose[c]	
	M_I	0.061±0.010			0.045	1.35±0.23
	M_{II}	0.121±0.016			0.038	3.15±0.41
	M_{III}	0.032±0.006			0.043	0.74±0.15
	M_{IV}	0.0053±0.0020			0.0078	0.68±0.25
	M_V	0.0065±0.0020			0.0097	0.66±0.20
	M_I/M_{III}	1.94±0.30	1.92±0.19[a]		1.05	1.9±0.3
	M_{II}/M_{III}	3.85±0.39	3.73±0.37[a]		0.89	4.3±0.4
	M_{IV}/M_{III}	0.17±0.04	0.1±0.012[a]		0.18	0.95±0.22
	M_V/M_{III}	0.21±0.04	0.12±0.014[a]		0.23	0.91±0.18

[a]Reference 17.

[b]Reference 25.

[c]Point-nucleus, unscreened value. Interpolation was made by using the values for 25.6 keV and 51.1 keV, given by Rose[26]), and the threshold value around 30 keV, given by O'Connell and Carroll[27]).

Table 8
Conversion coefficients of the E1 transitions from band D to band C

Transition energy (keV)	Shell	Exp	Theor (Sliv-Band)	Exp/theor
51.01	L_I	0.26±0.20	0.180	1.4±1.1
(D 1/2+ → C 1/2-)	L_{II}	0.33±0.23	0.188	1.8±1.2
	L_{III}	0.35±0.18	0.201	1.7±0.9
	L_I/L_{III}	0.80±0.30	0.90	0.9±0.3
	L_{II}/L_{III}	0.91±0.20	0.94	1.0±0.2
64.83	L_I	0.098±0.023	0.122	0.80±0.19
(D 1/2+ → C 3/2-)	L_{II}	0.125±0.025	0.096	1.33±0.26
	L_{III}	0.105±0.021	0.095	1.10±0.22
	L_I/L_{III}	0.92±0.15	1.29	0.71±0.12
	L_{II}/L_{III}	1.20±0.15	1.01	1.19±0.15

Table 9
M subshell conversion coefficients of the 13.81-keV transition

Subshell	Experimental ICC	Theoretical ICC[a]		Calculated ICC: M1 + 0.15% E2	
	relative	M1	E2	relative	absolute
M_I	100	6.9(2)	9.3(2)	100	691
M_{II}	15.6±0.3	7.3(1)	4.6(4)	20.6	142
M_{III}	8.5±0.4	3.2(0)	2.6(4)	6.1	42
M_{IV}	≤7.0 [b]	7.1(-1)	4.2(2)	0.19	1.34
M_V	≤4.4 [b]	3.9(-1)	1.6(2)	0.09	0.63

[a]Estimated from threshold values[27]); see sec. 10.

[b]The M_{IV} and M_V lines were incompletely resolved from the $L_3M_4M_5$ and $L_3M_5M_5$ Auger lines and our measured electron intensities were given as upper limits only.

Table 10
Photon transition probabilities from the 267.54-keV state (band C)

Transition	Multipolarity	Energy (keV)	Photon intensity	Partial half life (sec)		Hindrance factor F	$\lvert CG \rvert^2$
				Experiment	Single-particle estimate (Moszkowski)		
C 3/2- → B 5/2-	M1	208.00	23.0	2.2×10^{-8}	1.5×10^{-12}	1.1×10^{-4}	
C 3/2- → B 5/2-	E2	208.00	0.49	1.1×10^{-6}	2.9×10^{-9}	2.7×10^{-3}	0.571
C 3/2- → B 7/2-	E2	164.61	1.87	2.5×10^{-7}	9.5×10^{-9}	3.8×10^{-2}	0.429
C 3/2- → A 5/2+	E1	267.54	0.61	8.4×10^{-7}	3.5×10^{-15}	4.2×10^{-9}	
C 3/2- → A 5/2+	M2	267.54	0.15	3.3×10^{-6}	4.3×10^{-8}	1.3×10^{-2}	0.571
C 3/2- → A 7/2+	M2	234.40	0.021	2.4×10^{-5}	8.3×10^{-8}	3.5×10^{-3}	0.429

Table 11
Relative photon transition probabilities from the K=1/2+ band D.

Transition	Multipolarity	Energy (keV)	Photon intensity	Single-particle estimate for half-life (sec) (Moszkowski)	Hindrance[b] factor F (relative)	$\lvert CG \rvert^2$
D 1/2+ → C 3/2-	E1	64.83	1.25	2.5×10^{-13}	8.4×10^{-3}	0.667
D 1/2+ → C 1/2-	E1	51.01	0.22	5.0×10^{-13}	3.0×10^{-3}	0.333
D 1/2+ → A 5/2+	E2	332.36	1.29	2.8×10^{-11}	1.00	
D 3/2+ → A 5/2+	M1	370.94	0.12	2.6×10^{-13}	1.00	
D 3/2+ → A 5/2+	E2	370.94	$\lesssim 0.018$[a]	1.6×10^{-11}	8.8	0.571
D 3/2+ → A 7/2+	E2	337.72	0.0081	2.6×10^{-11}	6.6	0.429
D 5/2+ → A 5/2+	M1	368.59	0.050	2.8×10^{-13}	1.00	
D 5/2+ → A 7/2+	M1	335.38	0.102	3.6×10^{-13}	2.8	
D 5/2+ → A 5/2+	E2	368.59	$\lesssim 0.008$[a]	1.7×10^{-11}	$\lesssim 0.84$	0.214
D 5/2+ → A 7/2+	E2	335.38	$\lesssim 0.015$[a]	2.6×10^{-11}	$\lesssim 2.8$	0.508
D 5/2+ → A 9/2+	E2	292.7	0.0028	5.2×10^{-11}	1.0	0.278

[a]Obtained by using E2/M1 $\lesssim 0.15$ which is based on the measured K-internal conversion coefficients.
[b]These are only relative because of unknown life times of the relevant levels.

Table 12
^{237}U beta transition rates

Final state		Beta decay energy (keV)	Branching ratio (percent)	Log ft	Forbiddenness
Level energy (keV)	Spin and parity				
59.54	B 5/2-	455	<5	>8.3	1 h (B_{ij})
267.54	C 3/2-	248	43	6.6	1 u
281.35	C 1/2-	234	53	6.5	1 u
332.36	D 1/2+	183	3.0	7.3	ah
368.59	D 5/2+	146	<0.25	>8.1	2
370.94	D 3/2+	144	0.5	7.8	ah

Figure Captions

Fig. 1. Gamma-ray spectrum of ^{237}U above 150 keV taken with the 1 cm × 1 cm × 5 mm thick Ge(Li) spectrometer with FET preamplifier (B). A lead absorber of 400 mg/cm^2 thickness was used.

Fig. 2. Gamma-ray spectrum of ^{237}U and ^{241}Am taken with the 5 mmϕ × 3 mm thick Si(Li) spectrometer with FET preamplifier (C). A beryllium absorber of 50 mg/cm^2 thickness was used to stop electrons.

Fig. 3. Relative photopeak efficiencies of the solid-state gamma-ray spectrometers used in this study.

Fig. 4. Schematic view of the pre-accelerator system.

Fig. 5. L-subshell conversion electron lines of 208.00 keV transition, recorded with 50 cm $\pi\sqrt{2}$ iron-free spectrometer.

Fig. 6. Lines of fig. 5 plotted on semi-log paper after removal of background.

Fig. 7. L-subshell lines of 164.61 keV transition.

Fig. 8. Semi-log plot of lines of fig. 7 after background subtraction.

Fig. 9. M-subshell lines of 59.54 keV transition.

Fig. 10. Semi-log plot of lines of fig. 8 after background subtraction.

Fig. 11. M_I and M_{II} lines of 13.81 keV transition, observed with pre-accelerator system.

Fig. 12. Electron spectrum in region of M 26.35 and L 43.42, observed with pre-accelerator system.

Fig. 13. Decay scheme of ^{237}U. Photon intensities normalized to 100 beta disintegrations, are given in parentheses.

Fig. 14. Comparison of the experimental K conversion coefficients with the theoretical values of Sliv and Band.

Fig. 15. The experimental K, L_I, L_{II}, and L_{III} conversion coefficients of the 208 keV transition compared with theoretical values of Sliv and Band[24]), calculated as a function of M1 + E2 admixture.

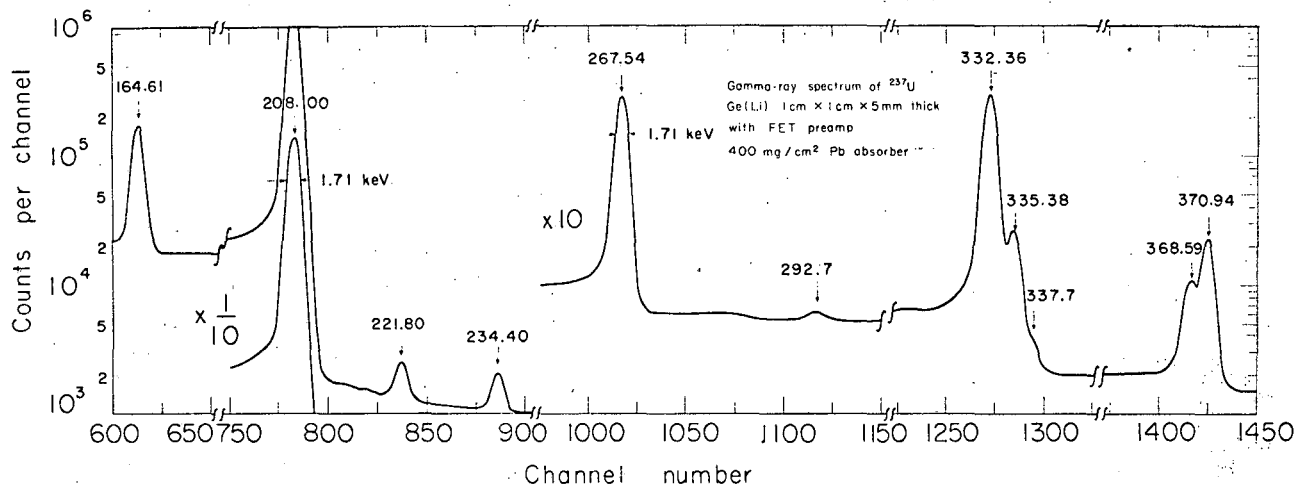
Counts per channel
Channel number
164.61
208.00
1.71 keV
x 1/10
221.80
234.40
267.54
1.71 keV
x 10
292.7
332.36
335.38
337.7
368.59
370.94
Gamma-ray spectrum of 237U
Ge(Li) 1cm × 1cm × 5mm thick
with FET preamp
400 mg/cm2 Pb absorber

Fig. 1

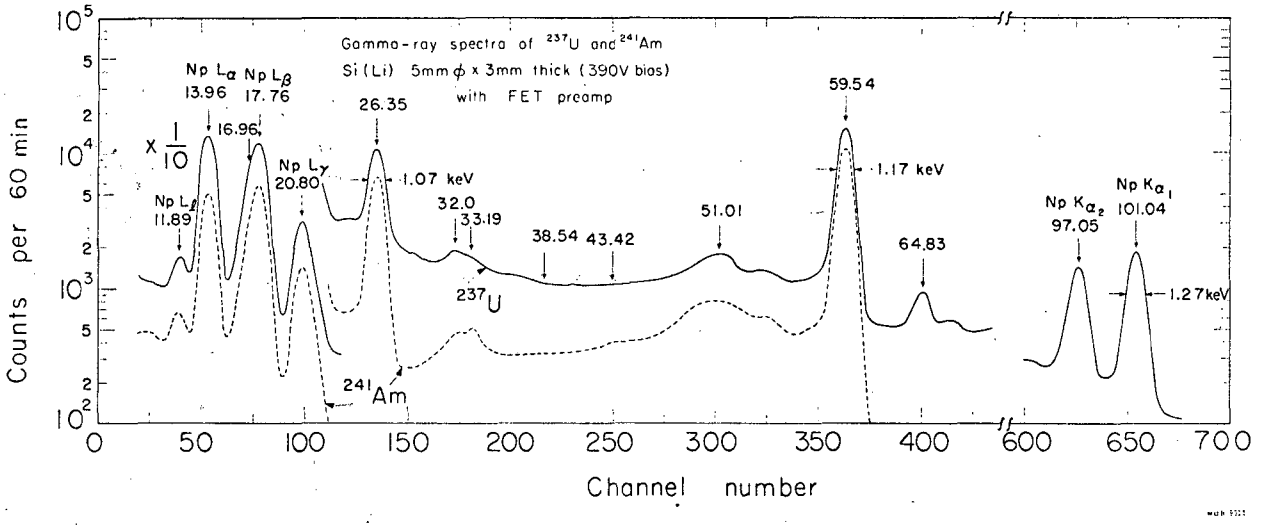
Gamma-ray spectra of 237U and 241Am
Si(Li) 5mm ϕ x 3mm thick (390V bias)
with FET preamp
Np Lα 13.96
Np Lβ 17.76
16.96
26.35
59.54
X 1/10
Np Lℓ 11.89
Np Lγ 20.80
1.07 keV
32.0
33.19
38.54
43.42
51.01
1.17 keV
64.83
Np Kα2 97.05
Np Kα1 101.04
1.27keV
237U
241Am
Counts per 60 min
Channel number

Fig. 2

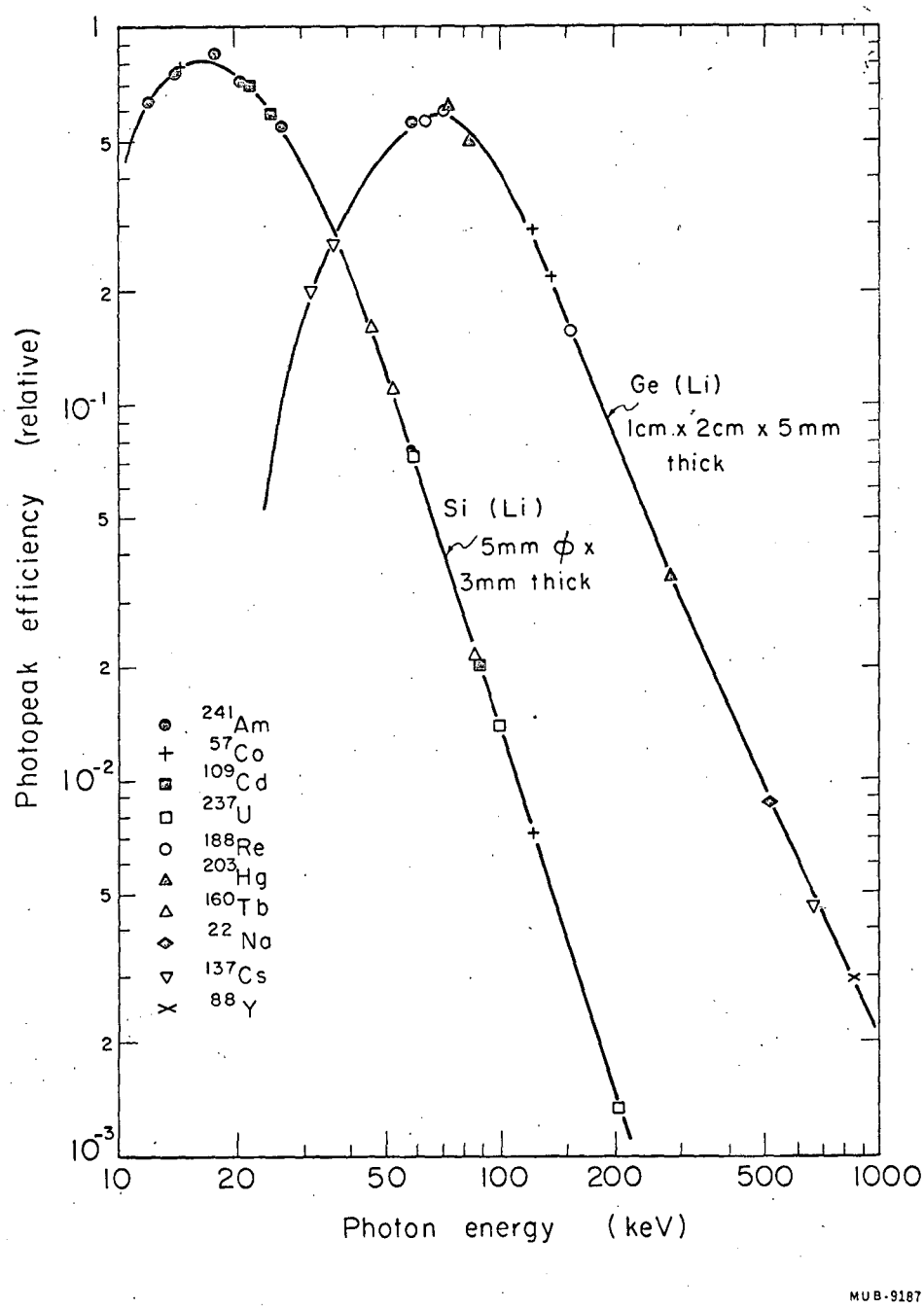
Photopeak efficiency (relative)
Photon energy (keV)
Ge (Li)
1cm x 2cm x 5mm thick
Si (Li)
5mm ϕ x 3mm thick
241Am
57Co
109Cd
237U
188Re
203Hg
160Tb
22Na
137Cs
88Y
MUB-9187

Fig. 3

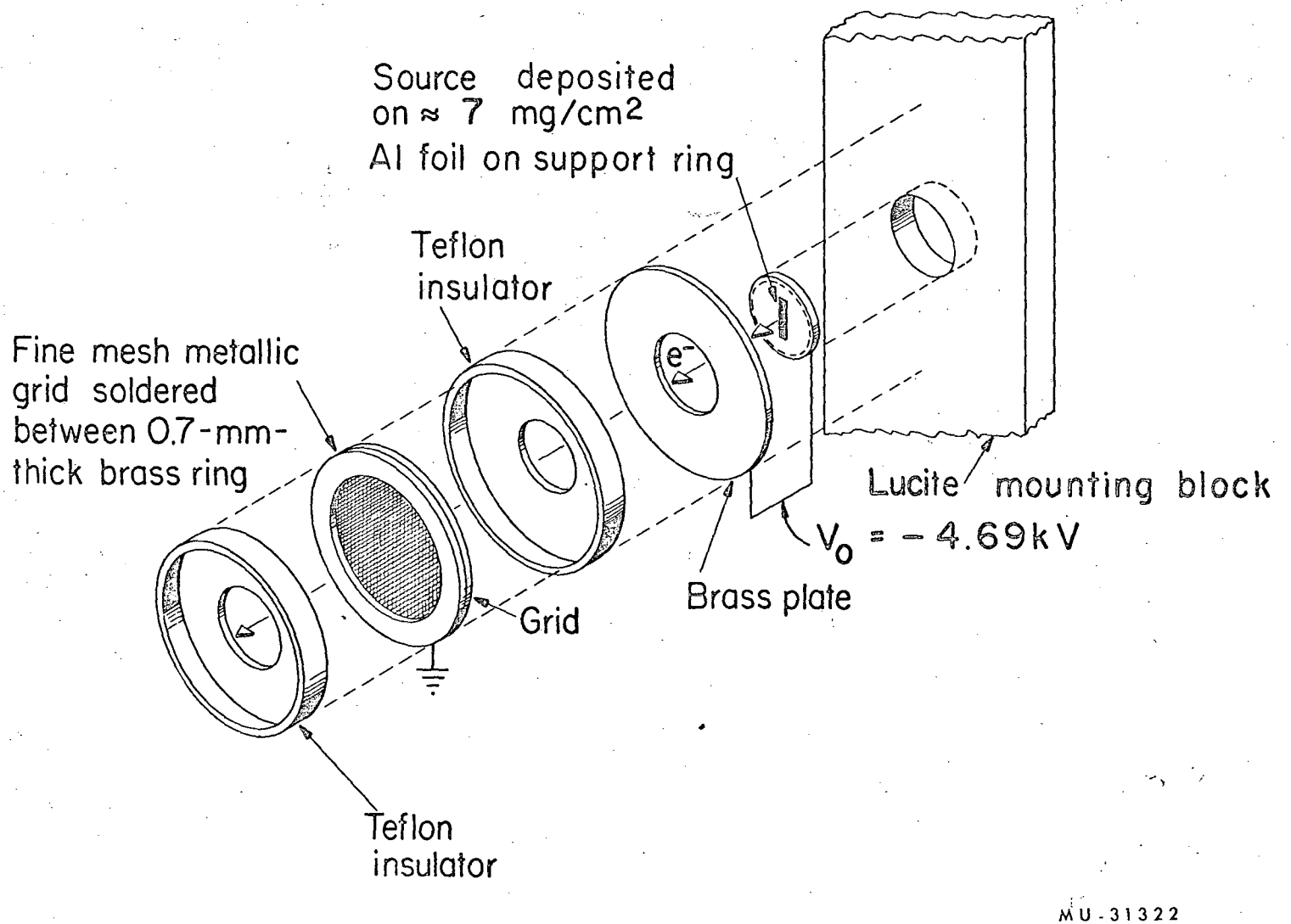
Source deposited
on ≈ 7 mg/cm2
Al foil on support ring
Teflon
insulator
Fine mesh metallic
grid soldered
between 0.7-mm-
thick brass ring
e-
Lucite mounting block
V0 = -4.69kV
Brass plate
Grid
Teflon
insulator
MU-31322

Fig. 4

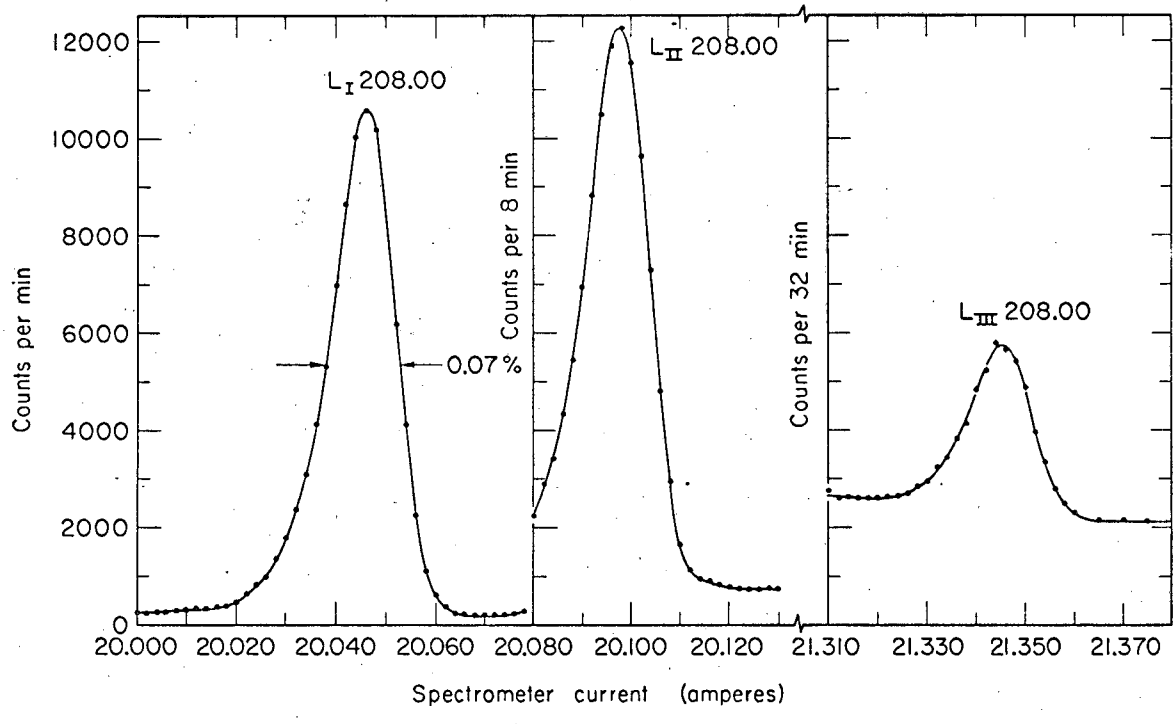
12000
10000
8000
6000
4000
2000
0
Counts per min
L_I 208.00
0.07%
Counts per 8 min
L_{II} 208.00
Counts per 32 min
L_{III} 208.00
20.000 20.020 20.040 20.060 20.080 20.100 20.120 21.310 21.330 21.350 21.370
Spectrometer current (amperes)
MUB-9173

Fig. 5

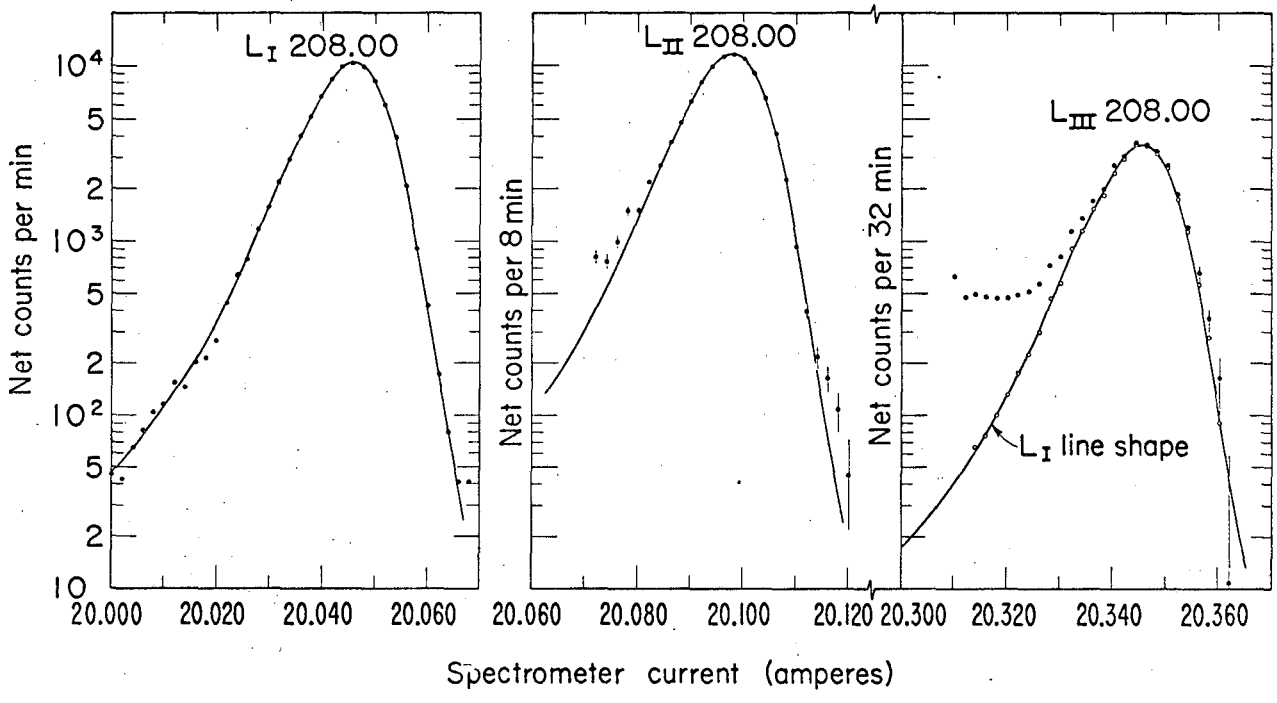
L_I 208.00
L_II 208.00
L_III 208.00
L_I line shape
Net counts per min
Net counts per 8 min
Net counts per 32 min
10⁴
5
2
10³
5
2
10²
5
2
10
20.000
20.020
20.040
20.060
20.060
20.080
20.100
20.120
20.300
20.320
20.340
20.360
Spectrometer current (amperes)

Fig. 6

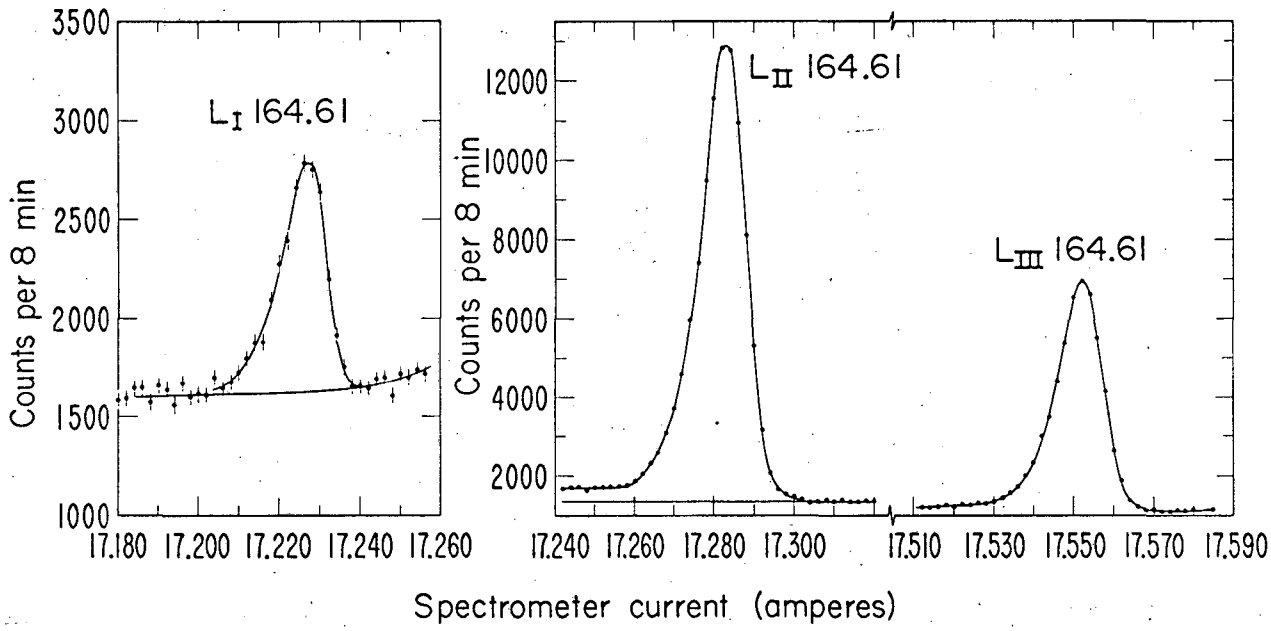
3500
3000
2500
2000
1500
1000
Counts per 8 min
L_I 164.61
17.180 17.200 17.220 17.240 17.260
12000
10000
8000
6000
4000
2000
Counts per 8 min
L_{II} 164.61
L_{III} 164.61
17.240 17.260 17.280 17.300
17.510 17.530 17.550 17.570 17.590
Spectrometer current (amperes)
MUB-9176

Fig. 7

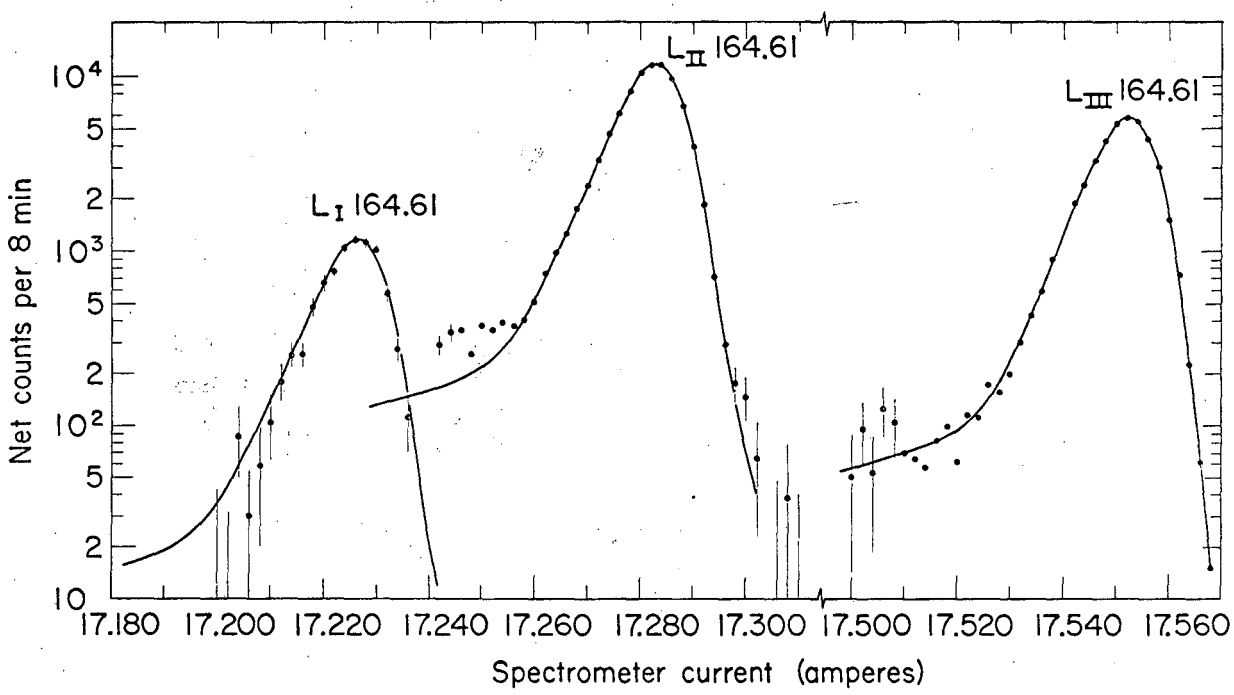
L_I 164.61
L_{II} 164.61
L_{III} 164.61
Net counts per 8 min
10^4
5
2
10^3
5
2
10^2
5
2
10
17.180 17.200 17.220 17.240 17.260 17.280 17.300 17.500 17.520 17.540 17.560
Spectrometer current (amperes)

Fig. 8

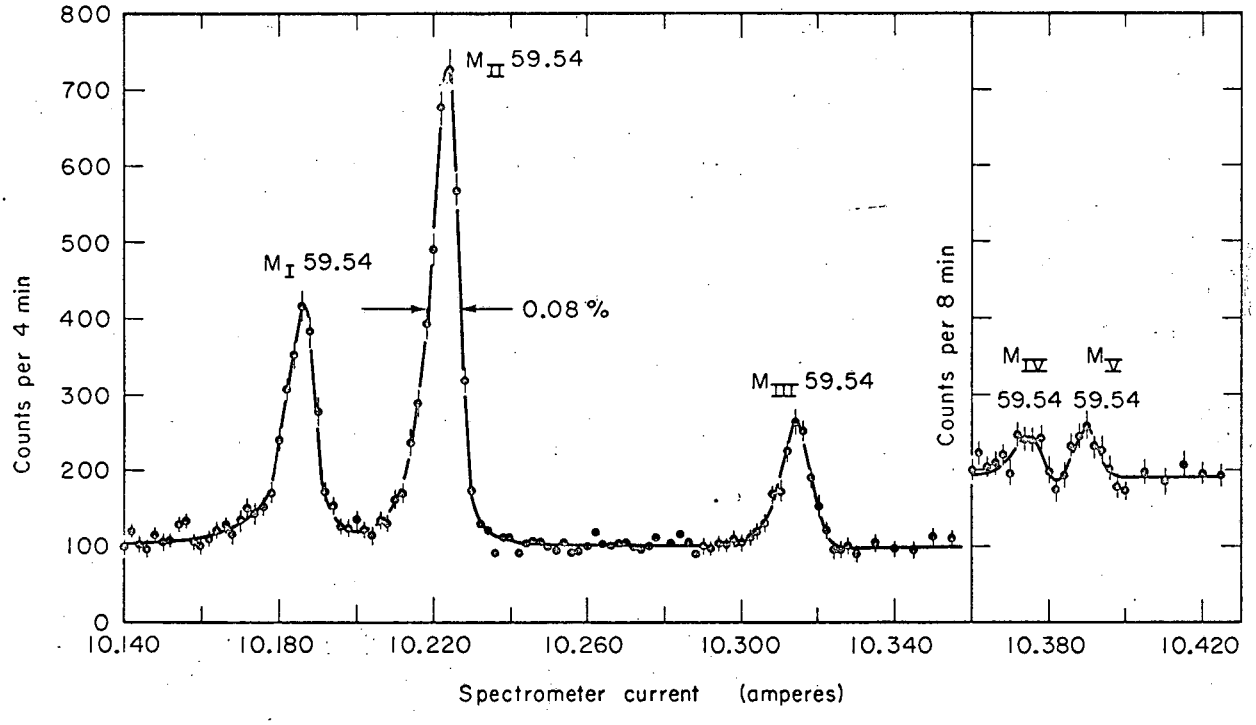
800
700
600
500
400
300
200
100
0
Counts per 4 min
Counts per 8 min
M_{II} 59.54
M_I 59.54
0.08 %
M_{III} 59.54
M_{IV} 59.54
M_V 59.54
10.140
10.180
10.220
10.260
10.300
10.340
10.380
10.420
Spectrometer current (amperes)
MUB-9172

Fig. 9

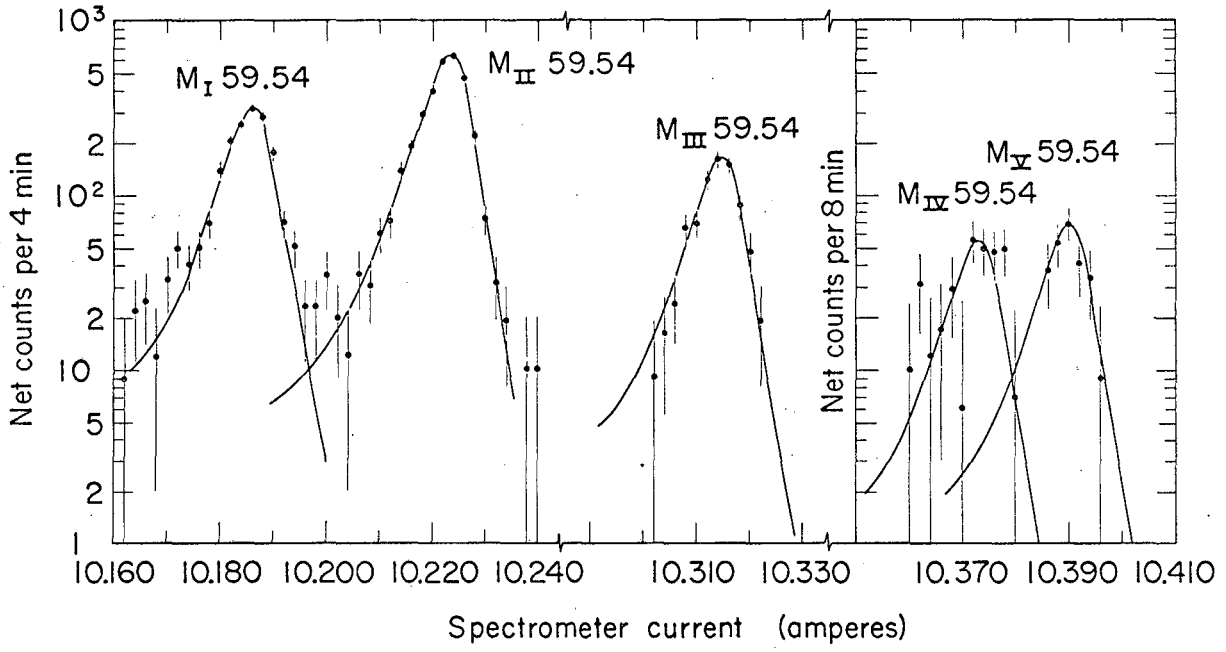
M_I 59.54
M_{II} 59.54
M_{III} 59.54
M_{IV} 59.54
M_V 59.54
Net counts per 4 min
Net counts per 8 min
10^3
5
2
10^2
5
2
10
5
2
1
10.160
10.180
10.200
10.220
10.240
10.310
10.330
10.370
10.390
10.410
Spectrometer current (amperes)
MUB-3175

Fig. 10

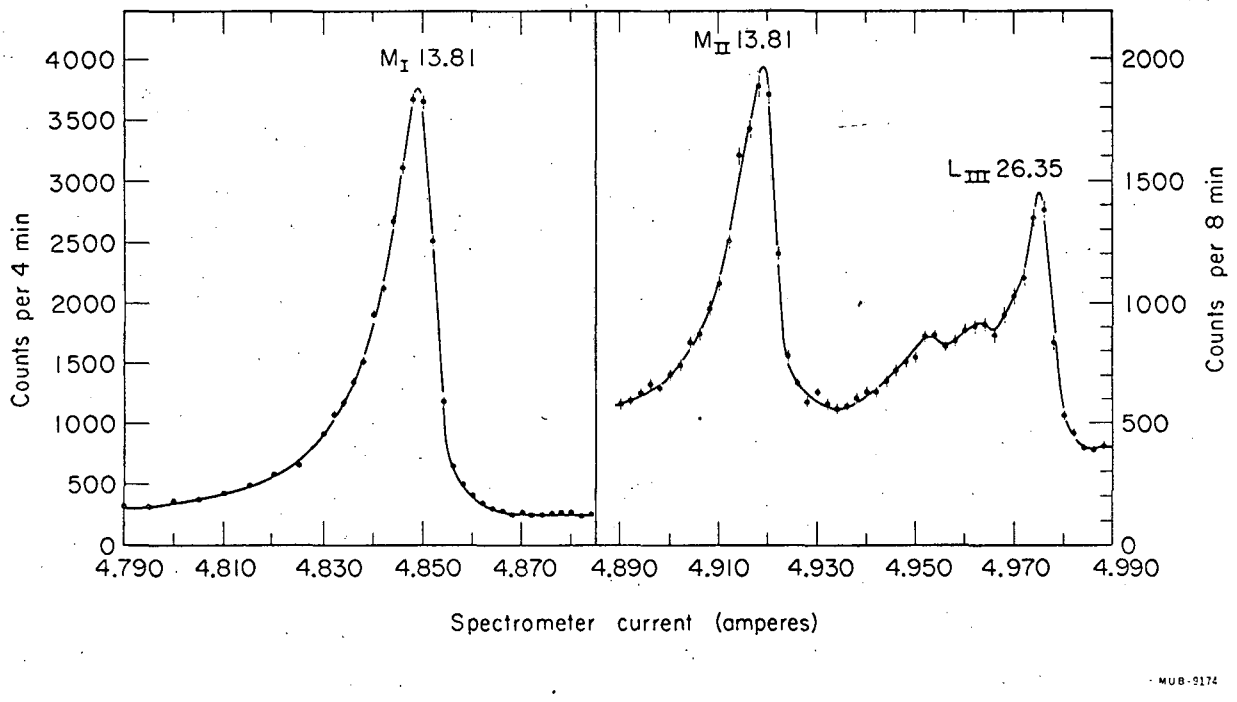
M_I 13.81
M_{II} 13.81
L_{III} 26.35
Counts per 4 min
Counts per 8 min
Spectrometer current (amperes)
4000
3500
3000
2500
2000
1500
1000
500
0
2000
1500
1000
500
0
4.790
4.810
4.830
4.850
4.870
4.890
4.910
4.930
4.950
4.970
4.990
MUB-9174

Fig. 11

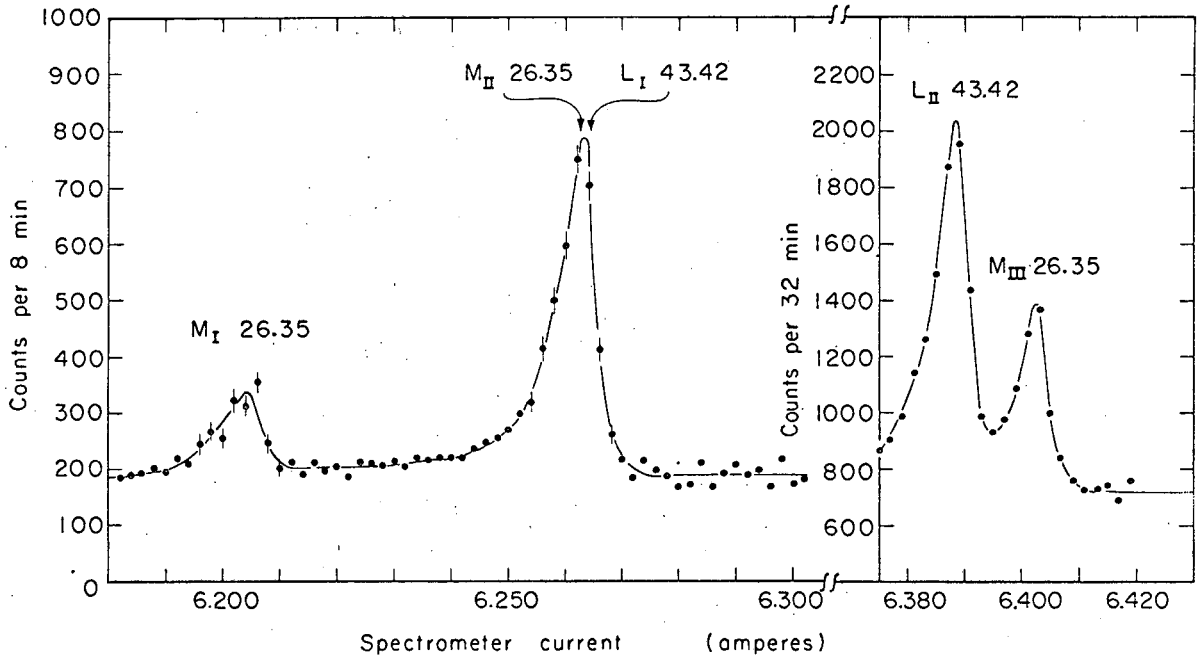

MUB-9093

Fig. 12

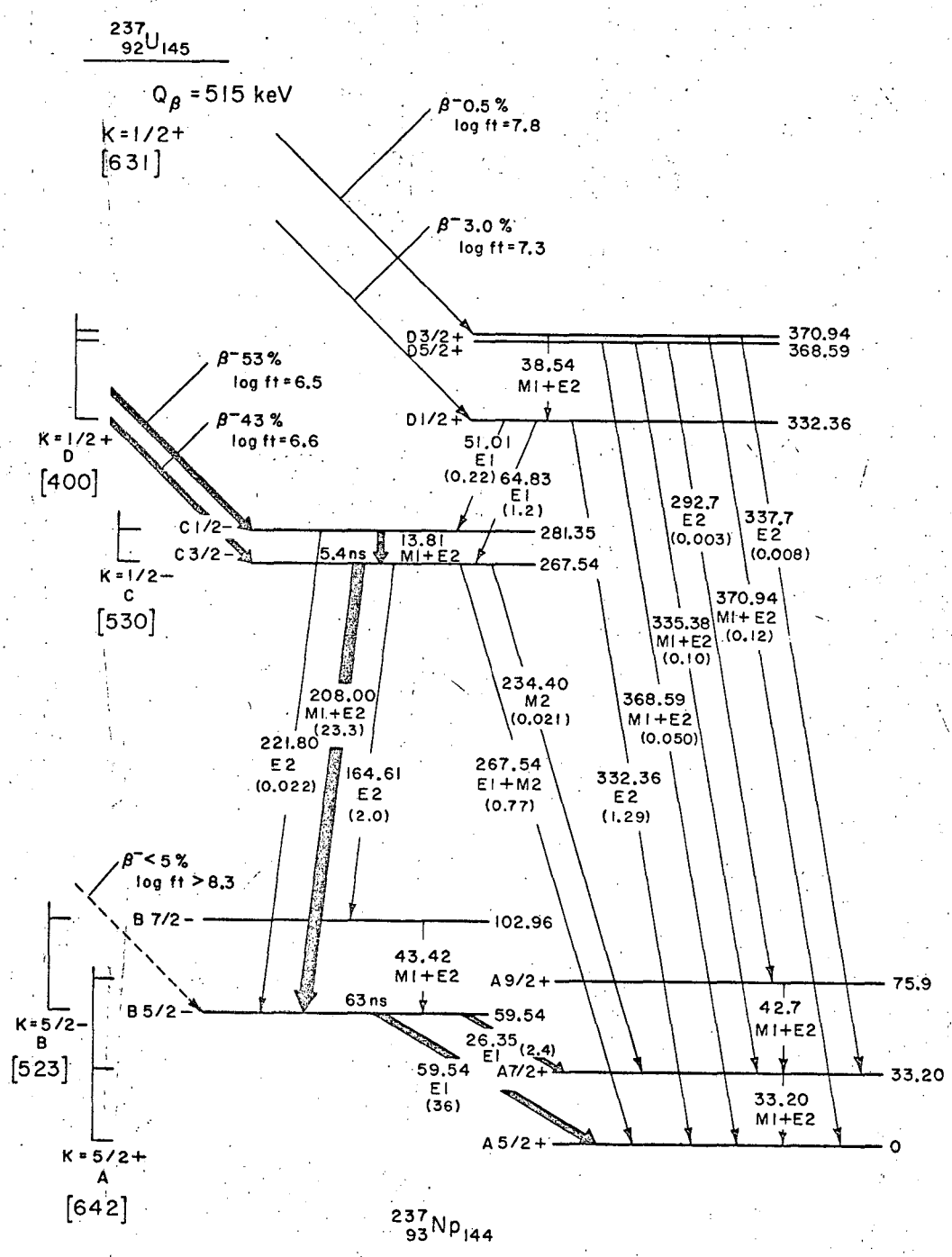
237 92 U 145
Qβ = 515 keV
K=1/2+
[631]
β⁻0.5 %
log ft = 7.8
β⁻3.0 %
log ft = 7.3
D 3/2+
D 5/2+
370.94
368.59
38.54
M1+E2
D 1/2+
332.36
β⁻53 %
log ft = 6.5
β⁻43 %
log ft = 6.6
K=1/2+
D
[400]
51.01
E1
(0.22)
64.83
E1
(1.2)
292.7
E2
(0.003)
337.7
E2
(0.008)
C 1/2−
281.35
C 3/2−
5.4ns
13.81
M1+E2
267.54
K=1/2−
C
[530]
370.94
M1+E2
(0.12)
335.38
M1+E2
(0.10)
234.40
M2
(0.021)
208.00
M1+E2
(23.3)
368.59
M1+E2
(0.050)
221.80
E2
(0.022)
164.61
E2
(2.0)
267.54
E1+M2
(0.77)
332.36
E2
(1.29)
β⁻< 5 %
log ft > 8.3
B 7/2−
102.96
43.42
M1+E2
A 9/2+
75.9
63ns
B 5/2−
59.54
42.7
M1+E2
K=5/2−
B
[523]
26.35
E1
(2.4)
59.54
E1
(36)
A 7/2+
33.20
33.20
M1+E2
A 5/2+
0
K=5/2+
A
[642]
237 93 Np 144
MUB-9171

Fig. 13

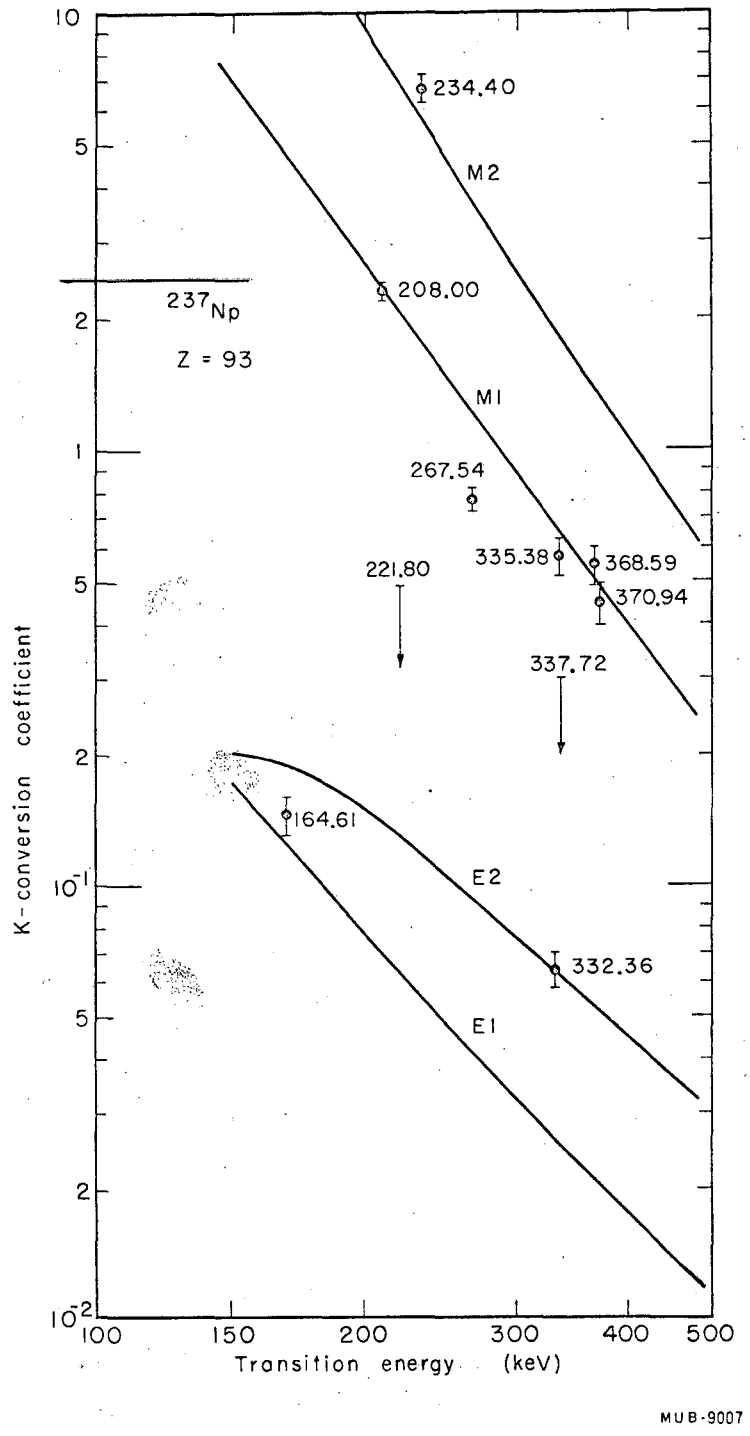
10
5
2
1
5
2
10^{-1}
5
2
10^{-2}
K-conversion coefficient
^{237}Np
Z = 93
234.40
M2
208.00
M1
267.54
335.38
368.59
370.94
221.80
337.72
164.61
E2
332.36
E1
100
150
200
300
400
500
Transition energy (keV)
MUB-9007

Fig. 14

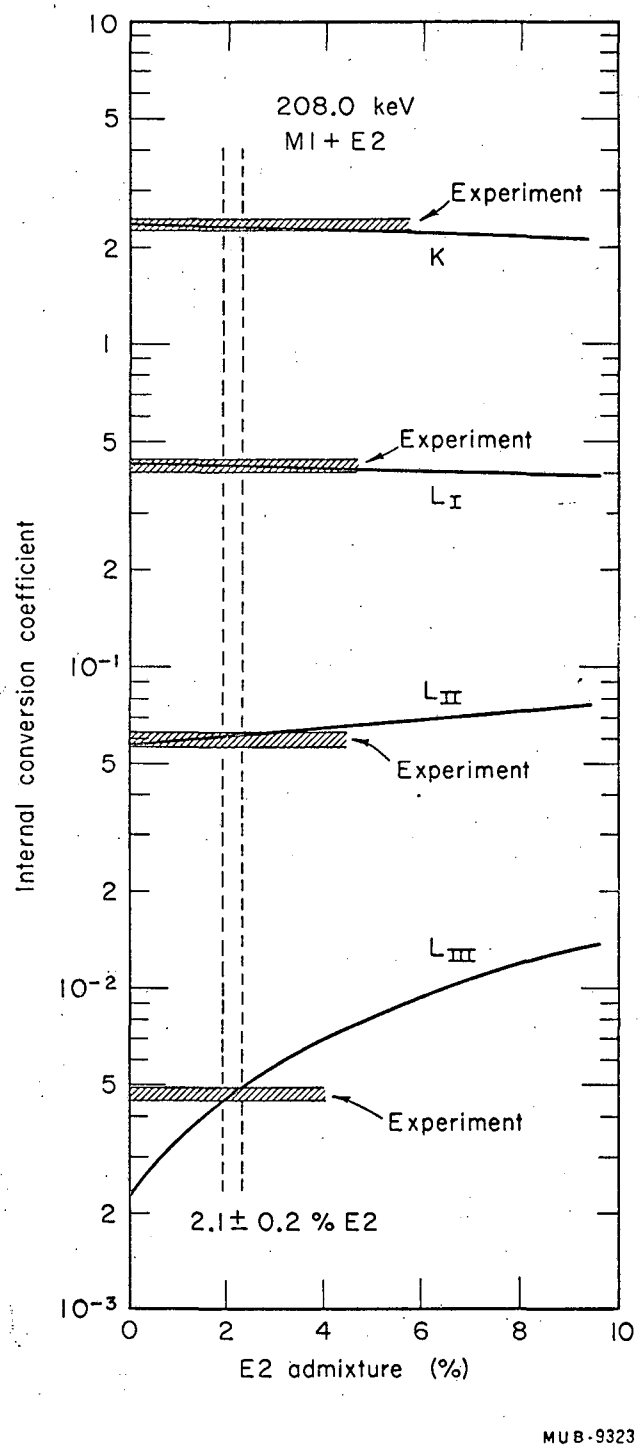
208.0 keV
M1 + E2
Experiment
K
Experiment
L_I
L_{II}
Experiment
L_{III}
Experiment
2.1 ± 0.2 % E2
Internal conversion coefficient
E2 admixture (%)
MUB-9323

Fig. 15

This report was prepared as an account of Government sponsored work. Neither the United States, nor the Commission, nor any person acting on behalf of the Commission:

A. Makes any warranty or representation, expressed or implied, with respect to the accuracy, completeness, or usefulness of the information contained in this report, or that the use of any information, apparatus, method, or process disclosed in this report may not infringe privately owned rights; or

B. Assumes any liabilities with respect to the use of, or for damages resulting from the use of any information, apparatus, method, or process disclosed in this report.

As used in the above, "person acting on behalf of the Commission" includes any employee or contractor of the Commission, or employee of such contractor, to the extent that such employee or contractor of the Commission, or employee of such contractor prepares, disseminates, or provides access to, any information pursuant to his employment or contract with the Commission, or his employment with such contractor.